

**Analysis of the structural determinants for
voltage-dependent G protein modulation of synaptic Cav2
channels**

by

Xuan Huang

A thesis

presented to the University of Waterloo

in fulfilment of the

thesis requirement for the degree of

Master of Science

in

Biology

Waterloo, Ontario, Canada, 2008

© Xuan Huang 2008

I hereby declare that I am the sole author of this thesis. This is a true copy of the thesis, including any required final revisions, as accepted by my examiners.

I understand that my thesis may be made electronically available to the public.

Abstract

Specialized voltage-gated calcium channels in the Ca_v2 channel class (such as $Ca_v2.2$, N-type) mediate neurotransmitter release from presynaptic nerve terminals. $Ca_v2.2$ channels are exquisitely sensitive to inhibition by G protein-coupled receptors. The ubiquitous form of G protein modulation is a fast, membrane delimited, voltage-dependent form of regulation, which is relieved by strong depolarizations. LCa_v2 , an invertebrate homolog from the pulmonate snail *Lymnaea stagnalis*, serves a similar function as a mediator of transmitter release in the nervous system. To examine the G protein modulation capacity in invertebrates, LCa_v2 was cloned to a bicistronic expression vector pIRES2-EGFP and expressed in HEK293T cells. Although LCa_v2 was almost indistinguishable from mammalian $Ca_v2.2$ in biophysical characteristics observed *in vitro*, snail LCa_v2 channel lacked the property of voltage dependent G protein modulation. The structural elements essential for the voltage sensitivity to G protein modulation were explored by swapping the N-terminus and I-II linker regions of $rCa_v2.2$ channels into LCa_v2 calcium channels. Functional comparisons were also made using both mammalian and invertebrate homologs of G protein beta subunits, $G\beta_1$. Neither the N-terminus or I-II linker region of $Ca_v2.2$ alone, nor the invertebrate G protein beta subunit was sufficient for voltage-dependent G protein modulation. Further analyses using chimeric channels and G protein subunits will be required to find the minimal structural determinants for voltage-dependent G protein modulation.

Acknowledgements

Another two years have passed. The moment finishing my thesis, I realized I would pack the luggage again and leave many new friends, and leave Waterloo, my third hometown.

I am grateful to meet so many nice and talented people here, from whom I could always get encouragements and supports. I want to thank my supervisor Dr. Spafford. He always tried his best to help me, providing suggestions, tolerating my endless mistakes and encouraging me to go further in the academic road. I have harvested a lot of pleasure participating in the real research life under his instructions. I want to thank all my labmates. Our lab had become one of the most enjoyable places because of the joy and warmth you brought to me. I want to thank Adriano especially, from whom I learned a lot. He never hesitated to help me, patiently and gently. He also set a good example for me how to help others in future. I also would like thank my committee members: Dr Dixon and Dr Heikkila for providing many good suggestions on my thesis.

Thank all my friends, especially Yili, Liang and Jin, who are always supportive and sharing my laughs and tears. Without you, I can not have the two years happy time through depression and frustration.

Last but not least, thank my parents who support my every decision. Anywhere and anytime, you are the people I could depend on.

Table of Contents:

List of Figures:	vii
List of Tables:	ix
List of Abbreviations.....	x
Chapter 1 Introduction.....	1
1.1 Voltage Gated Calcium Channels and Neurotransmitter release	1
1.2 Voltage Gated Calcium Channels	1
1.2.1 VGCC classification	2
1.2.2 VGCC structure	3
1.3 G proteins.....	11
1.4 G protein modulation of neuronal calcium channels	12
1.4.1 Voltage Dependent G protein modulation	13
1.4.2 Molecular determinants of Voltage Dependent G protein modulation.....	14
1.4.3 Other G protein regulatory mechanisms.....	15
1.5 An introduction to <i>Lymnaea Stagnalis</i>	19
1.6 G protein modulation of LCa_v2	19
Chapter 2 Material and Methods	25
2.1 Cloning WT LCa_v2 -IRES-EGFP and derived chimeras.....	25
2.1.1 Bacterial Strains and Cloning, Expression Vector.....	25
2.1.2 Plasmid Preparation	25
2.1.3 DNA purification	26
2.1.4 Polymerase Chain Reaction	27
2.1.5 Competent cell preparation and heatshock transformation.....	27
2.1.6 Quantification of Nucleic Acids, Agarose Gel Electrophoresis, DNA Ligation, DNA Digestion and DNA Dephosphorylation	28
2.1.7 QuikChange Mutagenesis.....	28
2.2 Expressions of calcium channels in mammalian cell lines.....	29
2.2.1 Mammalian Cell lines	29
2.2.2 Passage of HEK293T Cell Line.....	30
2.2.3 Calcium Phosphate Cell Transfection	30
2.2.4 Lipofectamine transfection.....	31
2.3 Electrophysiological Recordings.....	32
2.3.1 Solutions and Materials	32
2.3.2 Whole cell recording	33
2.3.3 Data analysis	34
Chapter 3: Results.....	38
3.1 Cloning and Expression of wild-type LCa_v2	38
3.1.1 Construction of WT LCa_v2 - EGFP plasmid	38
3.1.2 Transfection and Expression of LCa_v2 calcium channels	39
3.1.3 Biophysical comparisons of LCa_v2 and $rCa_v2.2$	40
3.2 LCa_v2 Calcium Channel Lacks Voltage Dependent G Protein Modulation.....	59
3.3 Calcium channel structures responsible for voltage-dependent G protein modulation	

.....	69
3.3.1 Construction of the <i>LCa_v2</i> chimera with a mammalian I-II linker (<i>L1_R2_L3_L4</i>) or mammalian N-terminus (<i>R1_L2_L3_L4</i>)	69
3.3.2 <i>LCa_v2</i> (<i>L1_R2_L3_L4</i>) and <i>LCa_v2</i> (<i>R1_L2_L3_L4</i>) chimeras lack the property of voltage dependent G protein modulation	72
Chapter 4 Discussion	91
4.1 G protein modulation of presynaptic <i>Ca_v2</i> calcium channels	91
4.2 Expression of invertebrate <i>LCa_v2</i> channel	92
4.3 <i>LCa_v2</i> appears to lack voltage dependent G protein modulation	95
4.4 N-terminus and I-II linker of <i>rCa_v2.2</i> alone did not confer voltage dependent G protein modulation to <i>LCa_v2</i> calcium channels	102
4.5 <i>LCa_v2</i> as a model to study VD/VI G protein modulation	103
4.6 Summary	104
Appendix	106
Appendix 1: List of primers	107
Appendix 2: List of original recording data	108
References:	109

List of Figures:

Figure 1: Physical coupling between calcium channel and synaptic vesicle docking/fusion apparatus.	6
Figure 2: The predicted membrane topology, subunit interactions and structure domains of the voltage-gated calcium channel complex	9
Figure 3: The model for voltage-dependent modulation of Ca_v2 calcium channel through G protein coupled receptors (GPCR) activation.	17
Figure 4: The time course of LCa_v2 current corresponding to GTP- γ S dialysis.....	23
Figure 5: Schematic illustration of whole cell mode patch clamp.....	36
Figure 6: Illustration of the cloning strategy to construct LCa_v2 gene into pIRES2-EGFP vector from 5' <i>RatCa_v2.1-LCa_v2</i> -pMT2 in pMT2 vector.	43
Figure 7: Restriction Digestion Map of WT <i>LCa_v2-IR-EGFP</i> , the final plasmid containing wild type <i>LCa_v2</i> gene in pIRES2-EGFP vector.	45
Figure 8: Immunostaining of LCa_v2 transfected HEK-293T cells.	47
Figure 9: Sample trace of LCa_v2 barium current.....	49
Figure 10: Sample ensemble current traces of LCa_v2 (bottom trace) elicited by voltage steps (top trace) when barium was the charge carrier.....	51
Figure 11: Current-voltage relationship comparisons of LCa_v2 and <i>rCa_v2.2</i> calcium channel homologs.....	53
Figure 12: Comparisons of the inactivation decay. Hold at -100mV, membrane potential stepped to +20mV for 450mS.....	55
Figure 13: Steady state inactivation curves for LCa_v2 and <i>rCa_v2.2</i> barium currents.	57
Figure 14: Sample trace of pre-pulse facilitation of LCa_v2 and <i>rCa_v2.2</i> with the exogenous expression of rat $G\beta 1\gamma 2$ subunits.	62
Figure 15: Histogram summarizing the paired-pulse facilitation (PPF) of invertebrate LCa_v2 and mammalian <i>rCa_v2.2</i> calcium channels.	65
Figure 16: Histogram illustrating the paired-pulse facilitation of mammalian <i>rCa_v2.2</i> and invertebrate LCa_v2 channels coexpressed with invertebrate G protein beta subunit $LG\beta_1$	67
Figure 17: Amino acids sequence alignment of N-terminus and I-II linker among rat Ca_v2 family (<i>rCa_v2.1</i> , <i>rCa_v2.2</i> and <i>rCa_v2.3</i>) and LCa_v2	73
Figure 18: Illustration of Cloning Strategy to Construct LCa_v2 (_{L1R2L3L4}) Chimera.....	75
Figure 19: Restriction digestion analyses of three plasmid clones to identify successful <i>SpeI</i> mutants from QuikChange Mutagenesis PCR (Stratagene) to create <i>SpeI</i> restriction sites.	77
Figure 20: Double digestion to confirm the successful construction of MSN-SfuI, with a newly created SfuI (isochizomer BstBI) restriction site in the LCa_v2 MSN-pGEMT shuttle plasmid.	79
Figure 21: Double digestion to confirm the cloning of shuttle vector LCa_v2 SBS-pGEMT.	81
Figure 22: Double digestion to confirm the I-II linker chimera LCa_v2 (_{L1R2L3L4}).	83
Figure 23: Illustration of Cloning Strategy to Construct LCa_v2 (_{R1L2L3L4}) Chimera.....	85
Figure 24: Double digestion to confirm the N-terminus chimera LCa_v2 (_{R1L2L3L4}).	87

Figure 25: Histogram summarizing the paired-pulse facilitation experiment for I-II linker chimera $LCa_v2(L1_R2_L3_L4)$ and N-terminus chimera $LCa_v2(R1_L2_L3_L4)$ 89
Figure 26: Sequence alignment of invertebrate (*Lymnaea*) $G\beta 1$ subunit and rat $G\beta$ subunit homologs (rat $G\beta 1-4$). 100

List of Tables:

Table 1: Classification of Voltage-gated Calcium Channel in mammalian cells..... 8
Table 2: Paired-Pulse Facilitation (PPF) ratios describing the voltage dependent G protein modulation of Ca_v2 channels, *LCa_v2* or *rCa_v2.2* in the presence and absence of co-expressed, exogenous rat Gβγ subunits. 64

List of Abbreviations

AID	Alpha Interacting Domain
5-HT	serotonin
cAMP	cyclic adenine monophosphate
CMV	cytomegalovirus
DHP	Dihydropyridin
DRG	dorsal root ganglia
EGFP	enhanced green fluorescent protein
EPSP	Excitatory Postsynaptic Potentials
GABA	γ -aminobutyric acid
GDP	Guanosine diphosphate
GIRK	G protein-activated inwardly rectifying potassium (channels)
GPCR	G Protein Coupled Receptors
GTP	Guanosine-5'-triphosphate
HEK293T	human embryonic kidney (cell line)
HVA	High Voltage Activated
IRES	internal ribosome entry site
LVA	Low Voltage Activated
NE	norepinephrine
PKC	Protein Kinase C
PPF	prepulse-dependent facilitation or paired-pulse facilitation
PTX	Pertussis Toxin
RGS	Regulator of G-protein Signaling
VGCC	Voltage Gated Calcium Channels

Chapter 1 Introduction

1.1 Voltage Gated Calcium Channels and Neurotransmitter release

Neurotransmitters are the information carriers and signal transducers for neurons. Neurotransmitters bind to diverse postsynaptic receptors and then mediate multiple processes such as emotions, learning and behaviors (Hyman, 2005). For example, γ -aminobutyric acid (GABA) and serotonin (5-HT) have been reported to be involved in nociceptive modulation (Fields et al., 1991) while glutamate, dopamine, as well as GABA impacts learning and memory in behavioral tasks (Myhrer, 2003). The mechanics of synaptic transmission between neurons has been widely studied (Figure 1): When a propagating nerve action potential arrives at the presynaptic terminal, the change of membrane potential causes the opening of Voltage Gated Calcium Channels (VGCC) in presynaptic membranes, which leads to the influx of calcium ions. The rise in calcium is sensed by special calcium binding proteins catalyzing the fusion of neurotransmitter vesicles with the presynaptic membrane, a process that leads to the release of neurotransmitter into the synapse cleft. After diffusing across the synapse to the post-synaptic neurons, neurotransmitters bind to their specific receptors activating downstream pathways (Hyman, 2005; Ziv and Garner, 2004). Concerning their essential roles, the structure and modulation of VGCC are the focus of many researchers.

1.2 Voltage Gated Calcium Channels

Calcium ions are important signal molecules and they play a critical role in modulating cell functions such as synaptic development, muscular contraction and setting the firing frequency of neurons (Catterall, 2000; Zamponi, 2005). Voltage-gated calcium channels

(VGCC) are membrane-spanning proteins that mediate calcium ion entry and respond to membrane depolarization. Channel subtypes were initially identified based on the sensitivity to different drugs and the distinct biophysical characteristics of currents with the help of specific blockers and agonists. The structure and function of calcium channels were better understood after the individual calcium channel genes were cloned (Dolphin, 2006).

1.2.1 VGCC classification

Ten mammalian genes of $\alpha 1$ subunit, the major pore forming subunit for VGCC, have been isolated, all displaying specialized functions and distributions. Based on the cDNA sequence similarity and amino acid conservation, VGCC could be divided into three major families: Ca_v1 channels (L-Type), Ca_v2 channels including $Ca_v2.1$ (N-type), $Ca_v2.2$ (P/Q-type), and $Ca_v2.3$ (R-type), and Ca_v3 (T-type). While the first two classes belonging to HVA (High Voltage Activated) calcium channels which are activated above the resting potential, Ca_v3 belongs to LVA (Low Voltage Activated) calcium channels active at rest (Dolphin, 2006; Ertel et al., 2000). As shown in Table 1, different calcium channels are associated with distinct biological functions, tissue distribution and pharmacological properties.

Among the multiple VGCC genes, only the Ca_v2 family is considered to be directly involved in neurotransmitter release. Blockade of VGCC with specific antagonists such as ω -conotoxin GVIA (ω -CTX) or spider toxin AgaIVA, will inhibit N- ($Ca_v2.2$) and P/Q-type ($Ca_v2.1$) calcium channels respectively, and will block synaptic transmission, suggestive of a direct role of these calcium channel subtypes with the synaptic release of neurotransmitter

(Takahashi and Momiyama, 1993; Wheeler et al., 1994). When synthesized peptide was injected into presynaptic neurons to disrupt the interaction between N-type ($Ca_v2.2$) calcium channel and synaptic core complex, the neurotransmitter release between paired synapses recorded by EPSPs (Excitatory Postsynaptic Potentials) was also inhibited, indicating that N-type calcium channels were required for neurotransmission (Mochida et al., 1996). Immunocytochemistry work indicated that both $Ca_v2.1$ and $Ca_v2.2$ channels were primarily clustered in synaptic terminals where they participated in the release of neurotransmitter at active zones (Westenbroek et al., 1992; Westenbroek et al., 1995).

1.2.2 VGCC structure

HVA Calcium Channels form a heteroligomeric complex composed of four subunits α_1 , α_2 , δ , β subunits and sometimes a γ subunit (Figure 2), while the primary pore forming α_1 subunit contains the minimal machinery for a functional channel (Arikkath and Campbell, 2003).

The core α_1 subunit, coding approximately 2000 amino acids (~212 kD), is composed of four repeat membrane spanning domains, each consisting of six transmembrane segments (labeled S1 through S6). Cytoplasmic linkers (I-II, II-III and III-IV linkers) connecting these four domains and the cytoplasmic N- and C-terminals are focal points for many specific intracellular protein interactions. The α_1 subunit is also the primary pore forming subunit mediating the calcium entry, containing the voltage sensor and many of the drug binding sites. For example, the fourth helix of each domain is highly positive charged to sense the membrane electric field and homologous glutamate residues in all four domains of the pore

region (in the reentrant extracellular loop connecting 5th and 6th helices) are involved in calcium ion selection. (Catterall, 2000; McCleskey, 1994; Tedford and Zamponi, 2006)

The ~55kD β subunit is the best understood auxiliary subunit. Vertebrates express four β subunit genes, each bearing multiple splicing isoforms. Although several isoforms could associate with the plasma membrane, the β subunit is a hydrophilic, intracellular protein without any transmembrane segments. The beta subunit associates with calcium channel α_1 subunits through the Alpha Interacting Domain (AID). AID binds to a deep hydrophobic groove in the guanylate kinase domain of beta subunits. Coexpression of the β subunit could modulate a lot of functions of VGCC including upregulating current densities and modifying current kinetics (Arikkath and Campbell, 2003; Catterall, 2000; Tedford and Zamponi, 2006). It was proposed that the β subunit promotes membrane expression of calcium channels by masking the endoplasmic reticulum retention signal in α_1 subunit (Bichet et al., 2000). The β subunit may also affect the G protein inhibition of calcium channels by disrupting their association (Campbell et al., 1995).

α_2 - δ subunits, around 170kD in total, are two peptides encoded by the same gene and connected by disulfide bonds. They are extensively glycosylated. α_2 subunit is located extracellularly anchored by a δ subunit. Four vertebrate α_2 - δ subunits genes have been identified. The coexpression of α_2 - δ subunits could enhance the peak current amplitude and alter the channel pharmacology (Arikkath and Campbell, 2003; Catterall, 2000; Tedford and Zamponi, 2006). Extracellular domains of α_2 - δ subunits have been shown to be responsible for increasing the drug binding affinity for the Ca_v1.2 calcium channel (Gurnett et al., 1997).

The γ subunit was thought to be only associated with skeletal VGCC but several recent

study revealed it might exist in the nervous system as well (Letts et al., 1998). However, compared to β and $\alpha_2\text{-}\delta$ subunits which are necessary for VGCC expression and function, γ subunit is not required for the integrity of the calcium channel (Arikkath and Campbell, 2003).

Figure 1: Physical coupling between calcium channel and synaptic vesicle docking/fusion apparatus. A high intracellular rise in calcium ion concentration is required for neurotransmitter release.

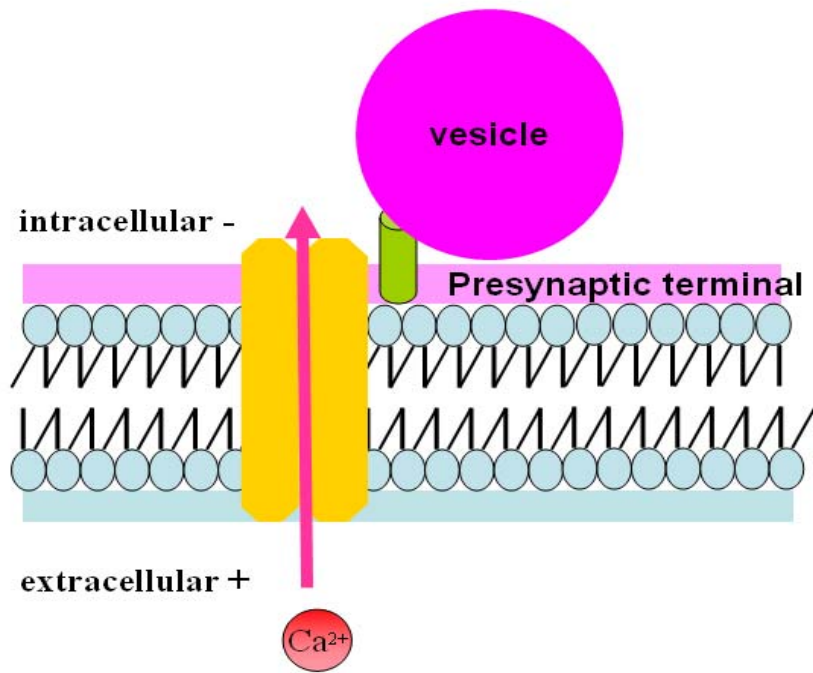
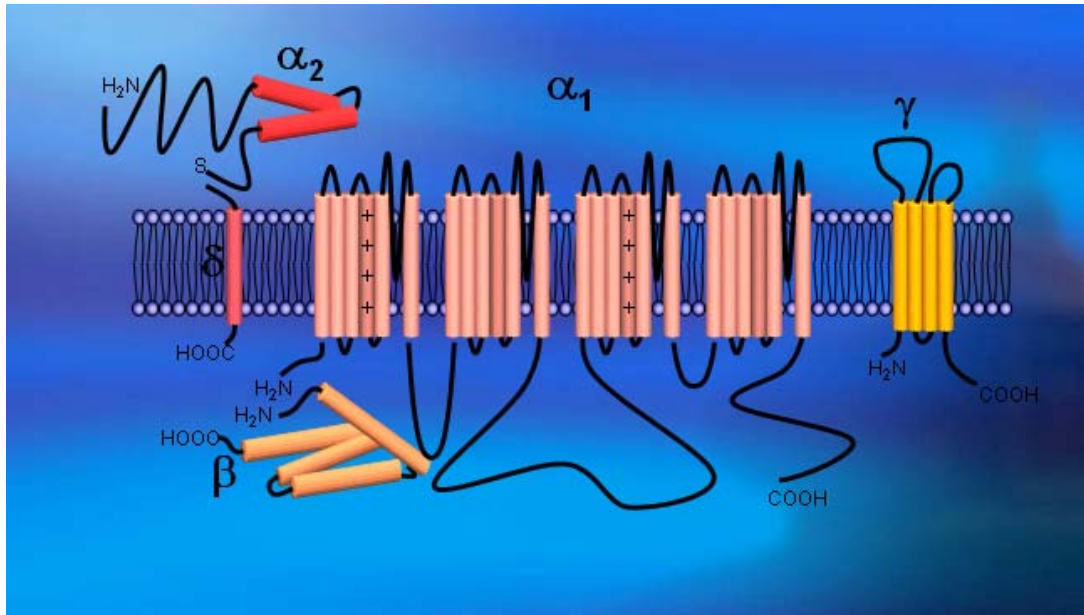


Table 1: Classification of Voltage-gated Calcium Channel in mammalian cells

Family	Nomenclature (α)	Current Type	Primary Tissue	Specific blocker	Function
Ca _v 1	Ca _v 1.1 (α_1S)	L-type	skeletal muscle	DHPs	Excitation-contraction coupling; calcium homeostasis; gene regulation
	Ca _v 1.2 (α_1C)		heart; brain; smooth Muscle; endocrine cells	DHPs	
	Ca _v 1.3 (α_1D)		Brain; endocrine cells	DHPs	Hormone secretion; gene regulation;
	Ca _v 1.4 (α_1F)		Retina		Tonic neurotransmitter release
Ca _v 2	Ca _v 2.1 (α_1A)	P/Q-type	Brain	ω -agatoxin	Neurotransmitter release; dendritic calcium release
	Ca _v 2.2 (α_1B)	N-type	Brain	ω -conotoxin	
	Ca _v 2.3 (α_1E)	R-type	brain; retina	SNX-482	Calcium dependent action potential; neurotransmitter release
Ca _v 3	Ca _v 3.1 (α_1G)	T-type	Brain	mibefradil, efonidipine (non-specific)	Control repetitive firing patterns; nociception; hormone secretion
	Ca _v 3.2 (α_1H)		brain; heart; kidney; liver		
	Ca _v 3.3 (α_1I)		Brain		

Summarized from (Catterall, 2000; Ertel et al., 2000; Newcomb et al., 1998; Tanaka and Shigenobu, 2005; Tsien et al., 1991)

Figure 2: The predicted membrane topology, subunit interactions and structure domains of the voltage-gated calcium channel complex



1.3 G proteins

G proteins are GTP binding proteins, belonging to the GTPase superfamily which serves to transduce cell-surface receptor signaling to cytoplasmic effectors. The G protein mediated signal pathway is a major mechanism to transduce the extracellular signals into intracellular responses. G proteins form a heterotrimeric $\alpha\beta\gamma$ complex composed of an α subunit of 39-46 kDa, a β subunit of 37kDa and a γ subunit ~8 kDa, each composed of a variety of genes. At rest, GDP is bound to the α subunit. Once activated, the GDP is replaced by GTP, which leads to the disassociation of $\beta\gamma$ subunits. Both α subunit and $\beta\gamma$ subunits can trigger downstream pathways. Signaling is terminated when the α subunit hydrolyzes GTP to GDP, and the $\beta\gamma$ and α subunits reform a heterotrimeric complex.(Hepler and Gilman, 1992)

According to the structural homology and target specificity of α subunit, G proteins are grouped into 4 main families: Gs, Gi, Gq and G₁₂. Among them, the Gi family, which down-regulates the adenylate cyclase, can be inhibited by pertussis toxin (PTX) (Hepler and Gilman, 1992). Although G α subunit determines the basic G protein type and widely regulates different protein targets, accumulating evidence indicates multiple roles of G $\beta\gamma$ subunits, including modulating ion channels and activating enzymes/secondary signaling molecules. Six G protein β and twelve G γ genes have been identified in mammals. $\beta\gamma$ subunits form a tight complex which can only be separated by extreme conditions, such as denaturation. The multiple combinations of different G protein subunits guarantee diversity and specificity in fine-tuning physiological mechanisms (Clapham and Neer, 1997; Hepler and Gilman, 1992; Wettschureck and Offermanns, 2005).

Extracellular signals including a large number of hormones, neurotransmitters,

chemokines, and sensory stimuli can activate the G protein signal pathway by binding to GPCR (G Protein Coupled Receptors), such as the β -adrenergic receptor, opioid receptor and dopamine receptor, which are key controllers of physiological processes. GPCR are ubiquitous in metazoans and share a common structure of seven transmembrane segments, with an extracellular amino terminus and an intracellular carboxy terminus. There is little sequence similarity between different GPCR families, which may utilize distinct structures and mechanisms to activate specific G proteins (Bouvier, 2001; Dolphin et al., 1999). Through GPCR, G proteins mediate signaling of diverse physiological functions, such as cardiac regulation through β -adrenergic receptor and muscarinic receptor by sympathetic and parasympathetic systems, insulin secretion inhibition through the α_2 -adrenergic receptor in pancreatic β cells, and inhibitory neurotransmitter release through GABA_B receptors (Wettschureck and Offermanns, 2005).

1.4 G protein modulation of neuronal calcium channels

Voltage Gated Calcium Channels can be regulated by multiple secondary messengers including cAMP and PKC. In addition, G proteins can directly modulate presynaptic VGCC. Activation of neurotransmitter-activated GPCRs negatively regulates Ca_v2 channel activity (Dolphin, 2003). Kathleen Dunlap and colleagues were the first to demonstrate that, neurotransmitters including norepinephrine (NE), γ -aminobutyric acid (GABA) and serotonin (5-HT) decreased calcium currents in cell bodies of embryonic chick dorsal root ganglion neurons (Dunlap and Fischbach, 1981) through a Pertussis toxin (PTX) sensitive G protein pathway (Holz et al., 1986) and the N-type calcium channel was the major target (Cox and

Dunlap, 1992). Later, neurotransmitter modulation of N-type and P/Q-type calcium channels was ubiquitously identified in cell bodies and presynaptic terminals. Despite intense investigation, the details of the various G protein modulation pathways and other secondary messenger regulation of calcium channels is not completely known (Dolphin, 1995; Dolphin, 2003; Hille, 1994).

1.4.1 Voltage Dependent G protein modulation

The major form for G protein modulation of VGCC is a voltage-dependent inhibition resulting in the change on opening probability and gating kinetics of Ca_v2 family members P/Q-type ($Ca_v2.1$) and N-type ($Ca_v2.2$). Its characteristics and mechanisms have been thoroughly investigated by several groups (Catterall, 2000; Dolphin, 2003; Dolphin et al., 1999; Tedford and Zamponi, 2006; Zamponi and Snutch, 1998) (Figure 3). Although there are many points of disagreement, some of the details of voltage-dependent G protein regulation are agreed upon: (1) Voltage-dependent G protein inhibition leads to a reduction of peak calcium current, slowing of activation and inactivation, and a positive shift in the current-voltage curve. The kinetic changes lead to a more pronounced inhibition at a less depolarized voltage. VGCC are considered to transfer from a “willing to open” state to a “reluctant to open” state under G protein modulation. (2) Treatment with pertussis toxin (PTX) usually abolishes transmitter-induced inhibition. Pertussis toxin catalyzes the ADP-ribosylation of specific G protein alpha subunits, such as G_i , G_o and G_t , preventing them from interacting with GPCRs. (3) Calcium current inhibition appears to occur via a membrane-delimited pathway. It was found that calcium channels enclosed in cell-attached

patches were not affected by G protein modulation when agonist was added to the extracellular bath solution which could only activate GPCR outside the cell-attached patch. These data suggested that diffusible cytoplasmic messengers were not required in a mechanism that likely involved direct coupling of calcium channels with G proteins (Shapiro and Hille, 1993). (4) G-protein-dependent inhibition is strongly voltage dependent and can be temporarily relieved after strong depolarizations. Since the introduction of a double pulse facilitation reported by Stephen Ikeda (Ikeda, 1991), the paired pulse method is widely applied to compare the peak current with a strong prepulse larger than 100mV and the peak current without the prepulse. The voltage-dependent relief of inhibition is often referred as prepulse-dependent facilitation or paired-pulse facilitation (PPF). (5) It is G $\beta\gamma$ subunits that mediate the voltage dependent G protein modulation. Injecting G $\beta\gamma$ subunits in neurons could mimic the inhibition caused by neurotransmitters (Herlitze et al., 1996; Ikeda, 1996) and G $\beta\gamma$ subunits were also shown to bind with calcium channels (De Waard et al., 1997).

1.4.2 Molecular determinants of Voltage Dependent G protein modulation

The understanding of the molecular mechanisms of voltage dependent G protein modulation was greatly enhanced by gene cloning of VGCC genes, and *in vitro* heterologous expression in *Xenopus* oocytes (De Waard et al., 1997; Page et al., 1998; Qin et al., 1997; Zhang et al., 1996) and mammalian cell lines (Agler et al., 2005; Zamponi et al., 1997). The conclusion from these studies is that the N-terminus, the I-II linker connecting the first and second domains (DI and DII), as well as the C-terminus were proposed to be vital motifs in voltage-dependent G protein modulation.

A G $\beta\gamma$ binding motif “QQIER” was identified in the I-II linker of Ca_v2.2 (α 1B, N-type) (Ikeda, 1996) and shown to associate with Ca_v2.1 (α 1A, P/Q-type) (De Waard et al., 1997). Electrophysiological investigations with chimeric channels between α 1A/ α 1B/ α 1C (Zhang et al., 1996) and between α 1B/ α 1E (Dolphin et al., 1999; Page et al., 1998) and mutations in α 1A (De Waard et al., 1997) suggested the I-II linker and the N-terminus were important for G protein modulation. One study reported that the C-terminal fragment of Ca_v2.3 (α 1E,R-type) had a G protein modulatory site (Qin et al., 1997) while chimeras between α 1A/ α 1B also suggested the involvement of the C-terminus (Zhang et al., 1996). However, most believe that the C-terminus plays an auxiliary role, if it has a role at all in voltage-dependent G protein modulation (Tedford and Zamponi, 2006). Some of the controversies may be attributed to the differences in cellular backgrounds for expression, choice of chimeras and varying amounts of voltage dependent and voltage independent G protein modulation. A most recent study (Aglar et al., 2005) proposed that the N-terminus was fundamental to voltage dependent G protein modulation and formed an calcium channel inhibitory module with the I-II linker.

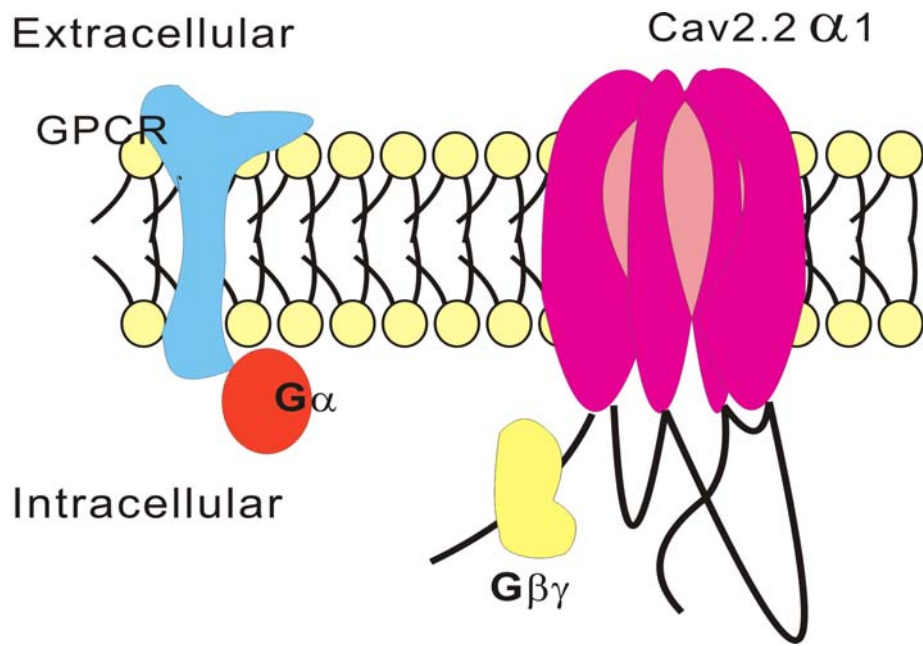
1.4.3 Other G protein regulatory mechanisms

Although the voltage-dependent pathway is widely spread, it is not the only way G proteins are known to regulate VGCC activity. It was suggested the inhibition of N-type calcium channels in rat superior cervical ganglion neurons was voltage independent and PTX-insensitive mediated through substance P activation while it was voltage dependent and PTX sensitive mediated by somatostatin (Shapiro and Hille, 1993). Intracellular application of PKC inhibitor could block the N-type inhibition produced by neuroepinephrine but not that

produced by GABA in embryonic chick sensory neurons (Diverse-Pierluissi and Dunlap, 1993) and it was proposed later, through different G protein subunits that both voltage dependent and voltage independent pathways participated (Diverse-Pierluissi et al., 1995). Micro-injection of an RGS protein (Regulator of G-protein Signaling) into dorsal root ganglion neurons, was reported to alter the tyrosine kinase mediated voltage independent G protein inhibition (Schiff et al., 2000). Application of GABA_B receptor agonist led to sequestering of calcium channels from the plasma membrane (Tomblor et al., 2006). This suggests an alternative explanation of voltage independent G protein regulation that may not involve alteration in calcium channel activity.

Recently, a specific, voltage-independent form of regulation was identified within a novel Ca_v2.2 isoform found only in nociceptive neurons in the dorsal root ganglia (DRG) neurons. This new splicing isoform contained a cell type specific 37a exon in the C-terminus of Ca_v2.2 and displayed the properties of both voltage-dependent and voltage-independent G protein modulation, while a unique tyrosine site might be responsible for its distinct voltage independent modulation property. Since ex37a is highly enriched in nociceptors, it might represent the natural adaptive response to pain (Bell et al., 2004; Ikeda and Dunlap, 2007; Raino et al., 2007).

Figure 3: The model for voltage-dependent modulation of Ca_v2 calcium channel through G protein coupled receptors (GPCR) activation.



1.5 An introduction to *Lymnaea Stagnalis*

The Mollusca is the second largest phylum in terms of the number of species. The large size and easy manipulation of neurons are widely appreciated properties while their membrane composition, ion channels and mechanisms of synaptic transmission do not differ in fundamental way from other invertebrates or even vertebrates (Chase, 2002). Nobel prize winners Hodgkin and Huxley used squid giant axon model to discover the ionic basis of membrane excitability (Hodgkin and Huxley, 1952) and Eric Kandel got the Nobel prize for his body of work that included mostly research on *Aplysia californica* (Kandel, 2004).

Lymnaea Stagnalis, a widely distributed holarctic animal inhabited in freshwater ecosystems, belongs to the subclass of Pulmonata within the class of Gastropoda, in the phylum Mollusca, superphylum Lophotrochozoa. All pulmonate snails bear pallial lungs, while non-pulmonate gastropods in aquatic ecosystems bear gills. Pulmonate snails rise to the water's surface to carry out gas exchange with the ambient air. The shell length of Lymnaeidae ranges from 2 to 6 cm. Although the dimensions of its central nervous system are small, the cells are highly pigmented and clearly visible. The nervous system of *Lymnaea Stagnalis* plays an important role in regulating respiration, blood circulation and water balance as well as controlling egg-laying behaviors (Chase, 2002).

1.6 G protein modulation of LCa_v2

Due to the complexity of mammalian VGCC genes and the difficulty to manipulate and work with identified neurons and synapses in mammals, invertebrates like *Lymnaea stagnalis* have become increasingly popular. *Lymnaea stagnalis* provides the following advantages for

neuroscience research. First of all, molluscs are part of the superclade lophotrochozoa which shares greater similarity with the human lineage in genome composition of nervous system related genes compared to the ecdysozoa which contains *Drosophila* and *C. elegans* (Moroz et al., 2006). Secondly, identified molluscan neurons are highly amenable for electrophysiological manipulation. Isolated neurons cultured *in vitro* could form robust synapses, while maintaining most of their *in vivo* characteristics (McCamphill et al., 2008; Spafford et al., 2003b). Moreover, invertebrates like *Lymnaea* bear only three versus ten mammalian calcium channel genes. *Lymnaea* has single representatives of the L-type calcium channel family (*L_{Ca_v1}*), non-L type family (homolog to N-type, P/Q-type and R-type) (*L_{Ca_v2}*), and a T-type calcium channel: (*L_{Ca_v3}*) (Spafford et al., 2003b). All three of these calcium channel genes have been isolated from *Lymnaea stagnalis*.

L_{Ca_v2a}, the major splice isoform in *Lymnaea*, is abundantly localized in presynaptic neurons and required for neurotransmitter release (Spafford et al., 2003b). Further, it was revealed that the biophysical characteristics of *L_{Ca_v2}* current *in vitro* were similar to those of mammalian presynaptic N-type calcium channels (Spafford et al., 2003a). Blockade of *L_{Ca_v2}* currents by treatment with GTP- γ S indicated that this channel could be modulated by G proteins like the N-type calcium channel (Spafford et al., 2003a). Serotonin was also shown to inhibit the presynaptic calcium currents through a G protein coupled pathway (McCamphill et al., 2008). However, the G protein modulation of *L_{Ca_v2}* is qualitatively different, as the inhibition of GTP- γ S could not be relieved by prepulses and was not reversible (Spafford et al., 2003a) (Figure 4). Preliminary investigations indicated that *Lymnaea* neuronal dihydropyridine-insensitive calcium currents in identified neurons and *L_{Ca_v2}* channels

expressed *in vitro* did not possess the mammalian-type voltage-dependent G protein modulation capacity.

The hypothesis of my proposed research is that LCa_v2 channels from *Lymnaea* do not possess the mammalian-type voltage-dependent G protein modulation capacity. Instead LCa_v2 calcium channel displays a unique voltage independent G protein modulation rather than the voltage dependent G protein modulation, providing a unique opportunity to study the necessary structural motifs for different forms of inhibition by G proteins.

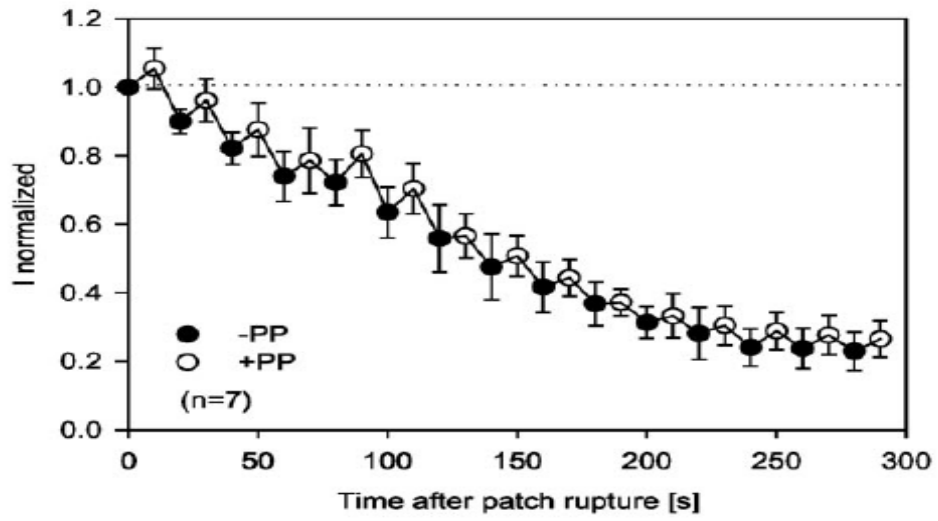
The goals of my research project are to:

- a) Prepare an LCa_v2 channel construct for heterologous expression in mammalian cell lines
- b) Characterize the biophysical properties of LCa_v2 calcium channels
- c) Compare the voltage-dependent G protein modulation of invertebrate LCa_v2 calcium channels and mammalian rat $rCa_v2.2$ calcium channels
- d) Compare the effectiveness of the *Lymnaea* G protein β_1 and mammalian G protein β_1 subunit in voltage-dependent G protein regulation
- e) Identify the structural determinants for voltage-dependent G protein modulation, by examining the functional consequences of swapping the cytoplasmic I-II linker and N-terminus from $rCa_v2.2$ into LCa_v2 channels

Calcium channel regulation is complex and fine-tuned for regulating nerve synapses. Multiple pathways involving a large repository of protein cascades coexist in presynaptic neurons to adjust activity of Ca_v2 channels. These provide a large number of possibilities to respond to various signals and regulate neuronal excitability and synaptic plasticity. My MSc

project tries to identify the structures in Ca_v2 channels that impart the unique G protein modulatory capacity.

Figure 4: The time course of LCa_v2 current corresponding to GTP- γ S dialysis. Currents were elicited by stepping from -100 mV to +20 mV, and every second test pulse was preceded by a depolarizing prepulse (*PP*) to +150 mV for 50 ms (*open symbols*). For each experiment, all current amplitudes were normalized to the peak current value seen with the first test pulse. Once GTP- γ S began to dialyzed into cytoplasmic solution after cell was ruptured, current amplitude decreased quickly, and could not be reversed by prepulses (Spafford et al., 2003a).



Chapter 2 Material and Methods

2.1 Cloning WT LCa_v2 -IRES-EGFP and derived chimeras

To study the characteristics of LCa_v2 calcium channel, wild type $LCav2$ gene was cloned into pIRES2-EGFP vector using the following techniques: plasmid preparation, PCR, DNA purification, DNA ligation, DNA transformation, clone selection, while chimeras with mutant nucleotides were constructed based on a QuikChange Mutagenesis method.

2.1.1 Bacterial Strains and Cloning, Expression Vector

E.coli DH5 α strain was the major bacterial strain used for cloning. While Stbl2 strain, derived from MAX Efficiency® Stbl2™ Competent Cells (SKU# 10268-019) from Invitrogen was used for cloning large fragments (above 5kb). Stbl2 cells were designed for cloning unstable inserts and are less likely to undergo recombination (recA minus). Different from 37 °C growing environment of DH5 α , Stbl2 cells were incubated at a lower 30 °C.

pIRES2-EGFP is the vector chosen for in vitro expression in mammalian cell lines. This plasmid contains a cytomegalovirus (CMV) promoter and a Kanamycin resistant gene. An internal ribosome entry site (IRES) was located between the multiple cloning sites and the coding region for enhanced green fluorescent protein (EGFP). To construct chimeras, a shuttle vector was derived based on pGEM-T which is a convenient cloning vector with an Ampicillin resistant gene.

2.1.2 Plasmid Preparation

Plasmid DNA was isolated by an alkaline lysis method separating the genomic DNA

from circular plasmid DNA. 3-5 ml overnight bacteria culture was spun down and resuspended in 100 μ l of Solution I (50 mM glucose, 25 mM Tris (pH=8.0), 10 mM EDTA). 200 μ l of Solution II (1% SDS, 0.2N NaOH) was added to the tube and mixed gently. Then 150 μ l of ice cold Solution III (3.0 M KOAC, 11.45 % (v/v) Glacial acetic acid) was added. After centrifugation, the plasmid DNA remains in the supernatant while other bacterial components including chromosomal DNA rested in the precipitant. RNase A (20 ug/ml) was added to prevent RNA contamination. 50:50 phenol/chloroform mixture was added and spun for 10 min to separate upper aqueous phase containing purified plasmid from contaminating proteins in the lower phase. Two volumes of 100% ethanol and sodium acetate to 0.3 M (1/10 volume of 3M sodium acetate) was added and spun for 10 minutes to pellet the plasmid DNA. DNA pellets were washed with 70% ethanol, air-dried, and resuspended in sterile water. Absorbance at OD260 was read on a UV spectrophotometer (Nanodrop ND1000) to quantify the purified plasmid DNA (1 OD unit = 50 ug/ml of dsDNA).

To isolate plasmids for transfection, GenElute HP Endotoxin-Free plasmid Maxiprep Kit purchased from Sigma-Aldrich (NA0400S, NA0400) was used to eliminate endotoxins which could hinder high transfection efficiencies.

2.1.3 DNA purification

DNA was re-purified between molecular biology protocols, such as after agarose gel electrophoresis, restriction enzyme digestion reactions, and DNA ligation reactions. Most DNA gel band purifications were carried out using a QIAquick Gel Extraction Kit (Cat No. 28704) purchased from Qiagen, or GFX PCR DNA and Gel Band Purification Kit (Lot

352860) purchased from GE Healthcare. Purifications of DNA gel band larger than 10kb required QIAEX II Gel Extraction Kit (Cat No. 20021) purchased from Qiagen or e.Z.N.A. Gel Extraction Kit (D2500-02) purchased from Omega.

2.1.4 Polymerase Chain Reaction

PCR (Polymerase Chain Reaction) was used to amplify DNA sequence for cloning and to carry out site-directed mutagenesis experiments. All primers are ordered from Sigma-Aldrich and dissolved in autoclaved MiniQ water as 100 uM and 20 uM working stock solutions. Information of all primers is listed in Appendix1. For a standard PCR using a thermocycler, DNA was first denatured at 94°C for 2min. Then DNA was denatured at 94°C for 30s, then annealed at 60°C for 45s, and elongated at 72°C for 1min, and repeated for 25-40 cycles. A final DNA elongation step was held at 72°C for 10min. PCR reagents such as Taq Polymerase were purchased from Fermentas. An Eppendorf Mastercycler EP silver block thermocycler was used for synthesizing DNA in the PCR reaction.

2.1.5 Competent cell preparation and heatshock transformation

To introduce ligation system or plasmid DNA into bacterial, chemical competent DH5 α and Stbl2 cells were prepared using a modified Hanahan protocol. Overnight culture was fed into 250 ml flask containing 100 ml of LB and grown until culture density reaches an OD600 spectrophotometric reading of ~0.5. Then bacterial pellet was gathered and resuspended gently in 16 ml of RF1 Solution (100mM Rubidium Chloride, 50mM Manganese Chloride, 30mM Potassium Acetate, 10mM Calcium Chloride, 15%w/v Glycerol, pH=5.8, filter

sterilized) and incubated on wet ice for 1 hour. Bacteria was pelleted and resuspended gently in 4 ml of RF2 Solution (10mM MOPS, 10mM Rubidium Chloride, 75mM Calcium Chloride, 15% (w/v) Glycerol) and incubated on wet ice for 15 minutes. Then 100 ul of chemically-competent cell suspension was dispensed into each pre-cooled microcentrifuge tubes and then quickly frozen in liquid nitrogen. Competent cells were able to take in DNA molecules using heatshock transformation.

2.1.6 Quantification of Nucleic Acids, Agarose Gel Electrophoresis, DNA Ligation, DNA Digestion and DNA Dephosphorylation

Nucleic acids were quantified using Thermo Scientific NanoDrop™ 1000 Spectrophotometer, which permits analyses with a 2 µl sample. Agarose gel electrophoresis for DNA was carried out at 1% to 2% agarose concentration in TAE buffer. New England Biolabs was the source of most enzymes used for molecular biology protocols, including: T4 ligase, restriction endonucleases and Antarctic Phosphatase for removing 5' phosphate groups from DNA. 1kb plus DNA ladder was purchased from Fermentas.

2.1.7 QuikChange Mutagenesis

QuikChange Mutagenesis was used to introduce DNA mutations of calcium channels to generate chimeras. In this procedure, the mutations were synthesized into DNA strands in the PCR with overlapping primers which incorporated the site directed mutations into a circular, nicked plasmid. The length and composition of the mutagenic primers were designed with the aid of *Stratagene's* web-based QuikChange® Primer Design Program, which is available

online at <http://www.stratagene.com/qcprimerdesign> and reaction was optimized using an experimentally-derived concentration of template (5ng, 10ng, 25ng, 50ng).

For QuikChange Mutagenesis PCR, a mixture of Vent and Taq Polymerase (1:20) was used and the PCR thermocycling protocol was modified as follows: DNA was denatured at 95°C for 2 min. For 12 cycles, DNA was denatured at 95°C for 30s, then annealed at 58°C for 1min, after which the DNA would be elongated at 72°C for 10min. Non-PCR generated plasmid DNA template from bacteria which is always methylated was selectively digested by DpnI. DpnI-resistant, PCR-mutagenized DNA was transformed into competent bacteria cells where the circularized plasmid was repaired of nicks and multiplied in dividing bacteria.

2.2 Expressions of calcium channels in mammalian cell lines

To characterize the LCa_v2 channel, wild type genes as well as chimeras were transfected into mammalian cell lines for expression.

2.2.1 Mammalian Cell lines

Rat and snail calcium channels as well as G-protein subunits harbored in mammalian expression vectors were heterologously-expressed, by transfecting into human embryonic kidney cell line (HEK293T) obtained from American Type Culture Collection (ATCC). HEK293T cells do not contain detectable levels of endogenous calcium channel subunits, serving as the appropriate surrogate for examining the *in vitro* expressed channels. The HEK293T is a highly transfectable derivative of the 293 cell line into which a stably plasmid containing the SV40 large T antigen is integrated. This maintains a high copy number of

plasmids expressed episomally, such as vectors used in my study (pCDNA, PMT2 or pIRES2) which contain the SV40 mammalian origin of replication.

2.2.2 Passage of HEK293T Cell Line

HEK293T (tsA-201) cells were grown in standard complete medium (DMEM supplemented with 1mM Sodium Pyruvate, 10%FBS, 50units penicillin and 50 μ g /ml streptomycin) as a monolayer in disposable culture flask to 85% confluency at 37°C in a CO₂ (5%) incubator. Every 3-4 days, 293T cells were passaged to a new flask by 1:6 dilution. To propagate the 293T cell line, cells were loosened from flask bottom with 0.5ml of trypsin, incubated at 37°C for 3-5 minutes before diluting in at least 1:10 complete media to inactivate the trypsin. Resuspended culture not used for maintaining the new passage were replated in 6 ml aliquots to 60 mm (diameter) sterile petri dishes containing 3 to 6 pre-sterilized poly-lysine coated glass coverslips (Circles No. 1 - 0.13 to 0.17mm thick; Size: 12mm, Fisher Scientific) for transfection and electrophysiology recording.

DMEM (Dulbecco's Modified Eagle's Medium, Cat No. 5796), sodium pyruvate solution (100mM, Cat. No. 8636), FBS (Fetal Bovine Serum Cat. No. F1051), Pen/Strep (5000 units penicillin and 5mg streptomycin/ml, Cat. No. P4458) and trypsin-EDTA (0.25%, Cat. No. T4049), were all purchased from Sigma-Aldrich Chemical Company. Fetal Bovine Serum was heat inactivated at 56°C for 15 minutes before use.

2.2.3 Calcium Phosphate Cell Transfection

Genes harbored in plasmids were introduced into HEK293T cells for protein expression

by standard calcium phosphate transfection method (Spafford et al., 2003a). In this technique, cells were split into 60mm dishes at approximately 50% confluency and settled for at least 3-4 hours before transfection. Around 10 µg of Plasmid DNA for transfection was added to sterile water to a final volume of 225 µl. 25 µl of 2.5M CaCl₂ was added to the DNA mixture then 250 µl of 2xHES buffer (280mM NaCl, 50mM Hepes, 1.5mM Na₂HPO₄· 7H₂O) was added drop by drop. Calcium phosphate crystals containing DNA plasmids would form after 20 minute incubation at room temperature before being applied on adherent HEK293T cells (in 4.5ml cell culture media). Calcium phosphate crystals were mixed in culture dishes plated with cells by gentle swirling and left to incubate overnight at 37°C in a CO₂ incubator. The next morning, cells were washed in PBS (137mM NaCl, 2.7mM KCl, 10mM Na₂HPO₄, 2mM KH₂PO₄, pH=7.2-7.4) three times and replaced with 6 ml of fresh media. Cells were allowed to recover from washing at 37°C for 2 hours then left in CO₂ incubator at a 30°C for at least 48 hours before patching. The lower 30°C temperature for incubation of cells promotes protein expression at the expense of cell division. In 100mm dishes, 20 µg of DNA, 50 µl of 2.5M CaCl₂, 500 µl of 2xHES buffer were used and the final transfection volume was 1ml, while cells were plated in 9ml complete media.

2.2.4 Lipofectamine transfection

Lipofectamine™ 2000 Transfection Reagent (11668-019) purchased from Invitrogen, is a proprietary cationic lipid formulation that offers high transfection efficiency and protein expression levels for HEK293T cells (Raingo et al., 2007). Based on the manufacturer's protocol, HEK293T cells were allowed to settle on coverslips in 60mm dish to 70%

confluency then the complete media was changed to 5 ml of non-antibiotic media before transfection. 20 μ l of lipofectamine reagent in 500 μ l of pure DMEM was mixed with 10 μ g of DNA which was also dissolved in 500 μ l of pure DMEM, and allowed to be incubated at room temperature for 10 minutes before adding the transfectant mixture to cell culture dishes.

2.3 Electrophysiological Recordings

Whole cell recording is an electrophysiological recording method to study the activity of ion channels in cell membranes.

2.3.1 Solutions and Materials

Calcium channel activities were measured by the whole-cell patch clamp technique. Transfected HEK293T cells were bathed and recorded in external solution containing barium as the charge carrier (20mM BaCl₂, 1mM MgCl₂, 10mM HEPES, 40mM TEA-Cl, 65mM CsCl, 10mM Glucose, adjust pH to 7.2 with TEA-OH, filter through 0.22 μ m filter). Barium is a preferred charge carrier because it passes through calcium channels more easily than calcium (currents in barium are twice as large as calcium) and barium does not activate/inactivate calcium-dependent intracellular signaling cascades. Ground electrodes were connected to the bath by a salt bridge, made from 5cm borosilicate glass (O.D.=1.5mm, I.D.= 0.086mm, item# = BF150-86-15) containing 2% agarose gel in 3M CsCl. Patch pipettes (2-5M Ω) are pulled from 7.5cm borosilicate glass (with filament, item# = BF 150-86-15) using a Model P-97 Flaming/Brown Micropipette Puller (Sutter Instrument Company) and polished using a MF-830 Micro Forge (Narishige, Japan). Patch pipettes were filled with

internal solution (108mM Cs-methanesulfonate, 4mM MgCl₂, 9mM EGTA, 9mM HEPES, adjust pH to 7.2 with CsOH, filter through 0.22µm filter), mimicking the components of cytoplasmic solution.

2.3.2 Whole cell recording

Whole cell patch clamp technique enables the analysis of the activity of ion channels in the cell membrane (Figure 5). Cells positively transfected with calcium channel subunits were identified by green fluorescence, emitted by EGFP either on the pIRES2-EGFP plasmid containing *LCav2* calcium channels, or on the pEGFP plasmid cotransfected. Green fluorescence was activated by mercury lamp on a Zeiss Axiovert 40 or 100 epifluorescence microscope with D455/70 nm band-pass filter. To carry out a recording, a patch of cell membrane was sealed and ruptured by the patch pipette with patch resistances between 2-5MΩ. Electrophysiological recordings were carried out in voltage-clamp mode at room temperature, where the membrane potential was clamped to a series of specified, commanded voltages by injecting current. In brief, the patch pipette was slowly lowered into the bath solution using a motorized manipulator until the pipette contacts with the cell membrane, yielding a slight increase in pipette resistance (~1 MΩ increase). Suction was then applied to patch pipette to form a gigaseal, with a pipette resistance above 1GΩ. When the gigaseal became stable, the cell was held at a holding potential of -100mV, and strong suction was applied to rupture the cell membrane under the patch pipette without breaking the seal at the edge of the glass-membrane interface.

Whole cell recordings were made with an Axopatch 200B amplifier (Axon Instruments,

Union City, CA), while monitored by the epifluorescence microscope (Axiovert 40 CFL, Zeiss). The voltage command generation and data acquisition were carried out using a PC computer equipped with a Digidata 1440A interface in conjunction with pClamp10 software (Molecular Devices). Recorded currents were filtered at 10 kHz using a low-pass Bessel filter and digitized at a sampling frequency of 2 kHz.

2.3.3 Data analysis

All data were stored as ABF extension form and off-line leak subtraction was carried out using ClampFit, an analysis program for electrophysiological data, when necessary. Figures were created in Origin 10, a professional data analysis and graphing software.

To observe the expression of calcium channels, a voltage step protocol for 450ms at +20mV from a -100mV holding potential was first applied to activate an inward barium current. For each single trial, the values of the current at every time points were collected, and normalized to the peak. The normalized data were averaged (Mean) then the standard errors (SE) were calculated. Data were illustrated as $\text{Mean} \pm \text{SE}$ to be plotted against the time points, where activation and inactivation were compared. The inactivation decay of the currents were exponential curve fit from just after peak current to current of maximal decay in the 450 ms step pulse. The exponential equation is $I=A1*\exp(-t/\tau)+A2$ where I is the normalized current amplitude, t is the time length after the peak and τ is the time constant for inactivation decay.

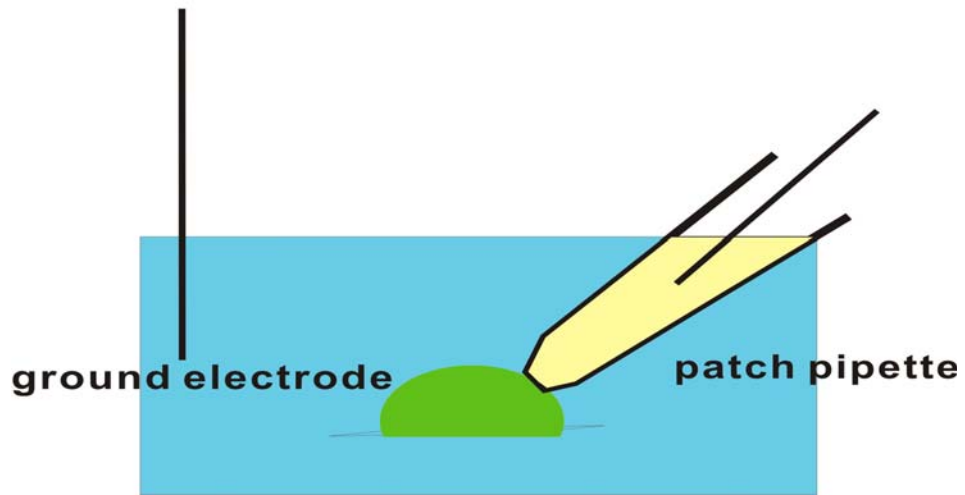
To characterize voltage sensitivities of the calcium channel, the current-voltage relationship was obtained by holding cells at -100mV before stepping to test potentials ranging from -50 to +60mV for 150ms. In each single trial, the values of peak current at each

holding potential were assembled together and normalized to the maximum. Normalized sets of data for each test were averaged (Mean), then the standard errors (SE) were calculated. The normalized peak currents were plotted to commanded voltages, generating the I-V relationship figure.

Steady state inactivation reflecting the voltage dependent of inactivation was also explored. Peak currents were examined at a test depolarization step to +20mV from -100mV holding potential, after 4s prepulse holding potentials ranging from -90 to +30mV. Values of peak currents after different prepulse holding voltage were collected and normalized to the maximum peak current. Then these normalized data were averaged and curve fit with a Boltzman equation $I=A1+A2/[1+\exp(V-Vh/S)]$ (Spafford et al., 2006) where I is the normalized peak current amplitude, V is the prepulse holding potential, Vh is the half-inactivation potential and S is a slope factor.

To study the voltage dependent G protein facilitation, paired pulse protocol was used to observe the prepulse facilitation. Facilitation was recorded by providing a +150mV strong depolarization lasting for 50ms, 25ms before the 40ms +20mV testing potential, while cells were held at -100mV. Facilitation was calculated by dividing the value of the peak current with a prepulse to the value of the peak current without a prepulse. Data among each group were averaged and illustrated as Mean \pm SE.

Figure 5: Schematic illustration of whole cell mode patch clamp. A coverslip plated with transfected HEK cells was placed in external solution in a 30mm dish. Positively transfected cells (green) were recorded with a glass pipette filled with internal solution. Currents were measured as the difference between the patch electrode and a ground electrode in the bath. Voltage clamp protocols were delivered by computer commands through Axopatch 200B (Axon Instruments) amplifier and a pCLAMP 10 software interface.



Chapter 3: Results

3.1 Cloning and Expression of wild-type LCa_v2

3.1.1 Construction of WT LCa_v2 -EGFP plasmid

An LCa_v2 calcium channel isolated from *Lymnaea stagnalis* and expressed *in vitro* previously was studied. The initial expression construct was a cDNA derived sequence contained in a pMT2 mammalian expression vector and the LCa_v2 N terminus was replaced by an N terminal sequence from $rCa_v2.1$ calcium channel, the P/Q type calcium channel isolated from rat, to boost *in vitro* channel expression on the membrane (Spafford et al., 2003a). Since critical cellular interactions were expected to involve the N-terminus, including G protein modulation, the first step in my project was to reclone LCa_v2 with the native N-terminus, and second, to transfer LCa_v2 into pIRES2-EGFP vector which was more amenable for selection of positive transfectants in mammalian cells than the pMT2 vector. pIRES2-EGFP is a bicistronic vector containing an internal ribosome entry site (IRES) between the multiple cloning sites containing the gene of interest (ie. LCa_v2 calcium channel) and the coding region for enhanced green fluorescent protein (EGFP). This enables the co-expression of calcium channel with the EGFP, whose fluorescent level could be visualized using an epifluorescence microscope.

The final LCa_v2 in pIRES2-EGFP plasmid (WT LCa_v2 -IR-EGFP) was constructed as followed (Figure 6): Step 1, 5' 2.2 kb from 5'*RatCa_v2.1*- LCa_v2 -pMT2 clone, the initial plasmid with a N-terminal sequence from $rCa_v2.1$ channel, was cut and ligated into a pIRES2-EGFP vector replacing a BarkCT (Carboxyl-Terminus of the Beta Adrenergic Receptor Kinase) gene, using an Sall restriction sites; 2, The N terminus from wild type

LCav2 sequence replaced the *rCa_v2.1* by insertion of a PCR product (XhoI-MluI) resulting in N-terminal 2.2 kb wild-type *LCa_v2* channel in pIRES2-EGFP (WT2.2-pIRES2-EGFP); 3, Most of the C-terminal 4.4kb sequence from 5' *RatCa_v2.1- LCa_v2-pMT2* clone was appended to N-terminal 2.2 kb fragment in pIRES2-EGFP using SacI restriction sites (SacI-*LCa_v2-pIRES2-EGFP*); 4, the C terminal 350bp sequence of *LCa_v2* was generated in the PCR from 5' *RatCa_v2.1- LCa_v2-pMT2* to create a compatible XmaI restriction site at the 3' end (SpeI-XmaI) (forward: Primer 1#, LCav2SpeIf; Backward: Primer 2#, LCav2CT-XmaI) into the pIRES2-EGFP plasmid.

After this series of cloning steps, the final plasmid was confirmed by restriction enzyme digestion (Figure 7). All PCR amplified sequences were confirmed by DNA sequencing. The length of full-length WT*LCa_v2-IR-EGFP* sequence is 11704 bp with insert of 6423 bp coding for *LCa_v2* gene encoding 2141 amino acids (GenBank: AAO83841).

3.1.2 Transfection and Expression of *LCa_v2* calcium channels

Due to the existence of many neuronal signaling pathways, the low endogenous calcium channel expression, and the easy accessibility for patch clamp, the HEK293T cell line was chosen for *in vitro* calcium channel expression (Berjukow et al., 1996; Thomas and Smart, 2005). HEK293T cells were transfected by calcium phosphate precipitation in 100 mm dishes with DNA plasmids encoding calcium channel subunits: either 8μg *LCa_v2* (pIRES2-EGFP) or 8μg *rCa_v2.2* (a rat α_1 subunit homolog) and <1 μg pEGFP were used, supplemented with 6μg *rβ_{1b}* (pMT2) and 6μg *rα_{2-δ}* (pMT2). The transfection of *rCa_v2.2* was supplemented with pEGFP because this gene was located in a pMT2 vector without a EGFP gene. In 60mm

dishes, the amount of transfected subunits were reduced to 3-4 μ g *L*Ca_v2 (pIRES2-EGFP) or *r*Ca_v2.2 and EGFP, 3-4 μ g *r* β _{1b} (pMT2) and 3-4 μ g *r* α _{2- δ} (pMT2). The expression level of EGFP correlated with the transfection efficiency and served as a marker for calcium channel subunit expression. According to the amount of cells with green fluorescence, the transfection efficiency was above 50%. 4-6 days after transfection, the cells were suitable for recording with enough expressed channels and good cell conditions. Biochemically, the expression of *L*Ca_v2 was detected by immunostaining using chicken anti-*L*Ca_v2 antibody which recognizes an extracellular epitope of *L*Ca_v2 (Figure 8). Electrophysiologically, the functional expression of *L*Ca_v2 could be assessed using a voltage step protocol during whole cell patch clamp recording (Figure 9). In brief, a quickly activated/inactivated inward barium current was generated when the cell was held at a depolarizing +20mV testing potential lasting 450ms while the resting potential was held at -100 mV.

3.1.3 Biophysical comparisons of *L*Ca_v2 and *r*Ca_v2.2

Both *L*Ca_v2 and *r*Ca_v2.2 are structural and functional homologs, which are localized in presynaptic neurons and play an essential role in synaptic transmission in snails (Spafford et al., 2003b) and mammals (Mochida et al., 1996). Despite their similarities in overall function, there are differences in structure. Alignment reveals only 43.6 % identity between the full-length isoforms of *L*Ca_v2 (2141 amino acids) and *r*Ca_v2.2 (2333 amino acids). 58% of amino acid residues are identical or highly similar to each other, and 33.4% are completely different in an alignment (ClustalW). To understand whether there is conservation in their biophysical properties, current-voltage relationship, inactivation decay and steady state

inactivation curve of LCa_v2 were characterized. For typical membrane ion channels, there are three different states: closed, open, and inactivated. Hold the membrane potential at resting potentials, most channels would be closed. When the membrane potential reaches a threshold, the channels would begin to open and mediate the passage of ions. Once activated to open, channels have a tendency to inactivate where the channels no longer respond to membrane potential changes and will not re-open, unless there is a strong membrane hyperpolarization which promotes the channels changing states from an inactivated state to a closed state. Current-voltage relationship, inactivation decay and steady state inactivation is to study the voltage dependent activation, time dependent inactivation and voltage dependent inactivation of channels respectively.

Current-voltage relations were generated using normalized peak barium current values, with a 150ms testing potential, stepping from -50mV to 60mV at 10mV intervals. A sample ensemble of traces is shown in Figure 10. Data from multiple cells were averaged and plotted as current-voltage relationships as shown in Figure 11. LCa_v2 and $rCa_v2.2$ have indistinguishable voltage-sensitivities: both start activating around -20mV and reach the peak at approximately +20mV.

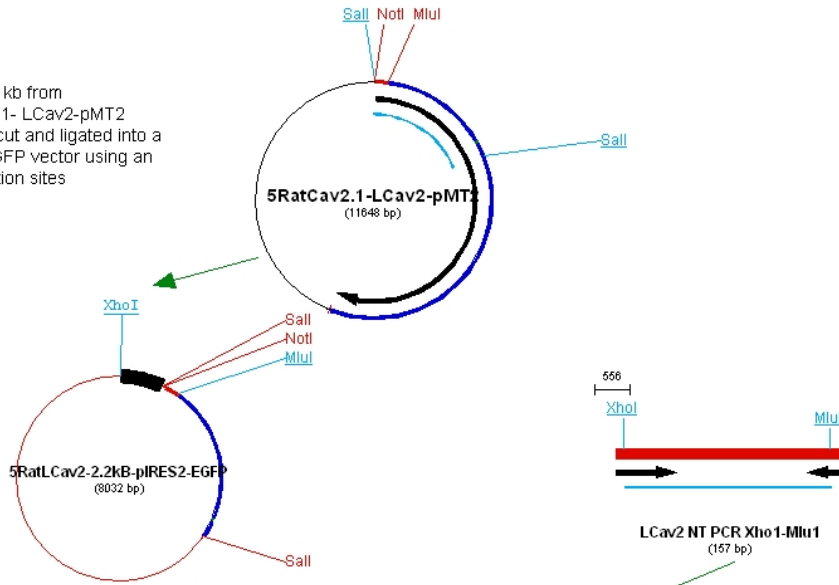
Peak current data can be used to estimate the kinetics of inactivation decay, quantified from just after the peak current value to the 450 ms time point where there is substantial inactivation of current (at least 70%) (n=7 or 8 different cells) (Figure 12). Exponential fit was applied to analyze the inactivation decay, with R values of 0.98165 and 0.99675 for LCa_v2 and $rCa_v2.2$ respectively indicating successful fittings. Compared to $rCa_v2.2$, inactivation rate of LCa_v2 was faster. The time constant (τ inact) for LCa_v2 was $43.2 \pm$

1.22ms (mean \pm SE) while that for $rCa_v2.2$ was 130.6 ± 0.85 ms. Activation rates also appeared to be a faster for LCa_v2 .

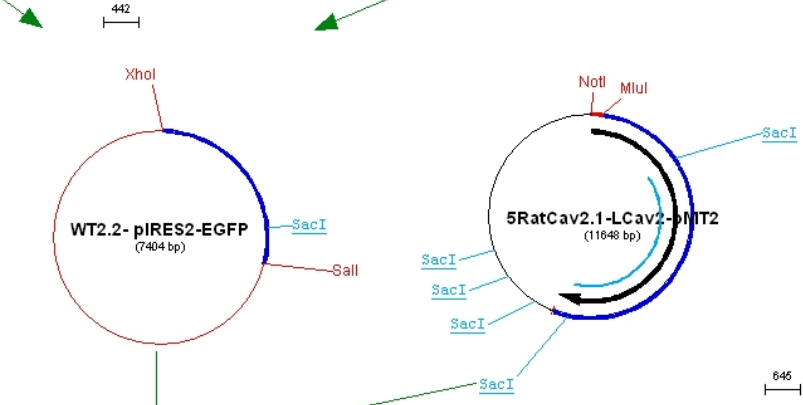
The voltage-sensitivities for inactivation were explored by steady-state inactivation. In this protocol, cells are held at holding potentials ranging from -90mV to 50mV for 4s until a steady-state fraction of calcium channels undergoing inactivation is achieved. This is followed by a voltage step to +20mV for 150ms in duration to measure the residual channels that are available for opening at a steady state. Normalized current values of steady state inactivation were plotted to the 4s prepulse holding potentials. A Boltzmann fit of the steady-state inactivation curve (Figure 13) indicated that LCa_v2 was half inactivated around -40mV while the half inactivation potential was -50mV for $rCa_v2.2$.

Figure 6: Illustration of the cloning strategy to construct *LCa_v2* gene into pIRES2-EGFP vector from 5' *RatCa_v2.1-LCa_v2-pMT2* in pMT2 vector. Step 1, 5' 2.2 kb from 5'*RatCa_v2.1-LCa_v2-pMT2* clone was cut and ligated into a pIRES2-EGFP vector using an *Sall* restriction sites; Step 2, The N terminus from wild type *LCav2* sequence replaced the *rCa_v2.1* by insertion of a PCR product (*XhoI-MluI*) resulting in WT2.2-pIRES2-EGFP; Step 3, Most of the C-terminal 4.4kb sequence from 5'*RatCa_v2.1- LCa_v2-pMT2* clone was appended to N-terminal 2.2 kb fragment in pIRES2-EGFP using *SacI* restriction sites (*SacI-LCa_v2-pIRES2-EGFP*); Step 4, the C terminal 350bp sequence of *LCa_v2* was generated in the PCR from 5'*RatCa_v2.1- LCa_v2-pMT2* and cloned into the pIRES2-EGFP plasmid using *SpeI* and *XmaI* restriction sites. Restriction sites chosen for cloning are colored in blue. Inserted fragments for each ligation reaction are marked by blue line. This illustration was created using Gene Construction Kit software (Textco).

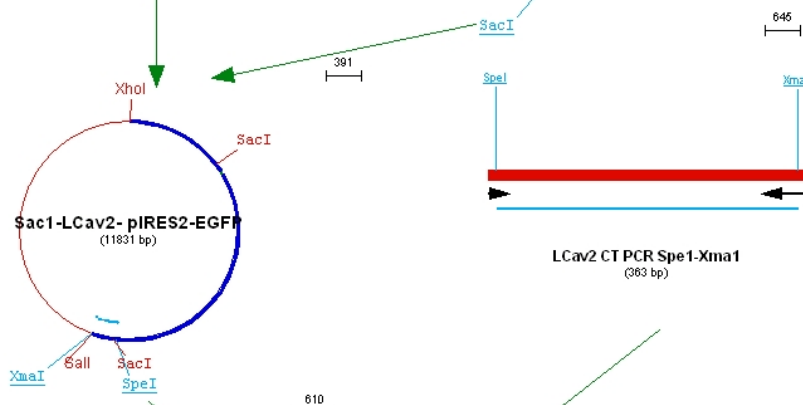
Step 1: 2.2 kb from 5'RatCav2.1- LCav2-pMT2 clone, was cut and ligated into a pIRES2-EGFP vector using an Sall restriction sites



Step 2: The N terminus from wild type LCav2 sequence replaced the RatCav2.1 by insertion of a PCR product (XhoI-MluI) resulting in N-terminal 2.2 kb wild-type LCav2 channel in pIRES2-EGFP (WT2.2-pIRES2-EGFP)



Step 3: Most of the C-terminal 4.4kb sequence from 5'RatCav2.1- LCav2-pMT2 clone was appended to N-terminal 2.2 kb fragment in pIRES2-EGFP using SacI restriction sites (SacI-LCav2-pIRES2-EGFP)



Step 4: the C terminal 350bp sequence of LCav2 was generated in the PCR from 5'RatCav2.1- LCav2-pMT2 to create a compatible XmaI restriction site at the 3' end (SpeI-XmaI) into the pIRES2-EGFP plasmid.

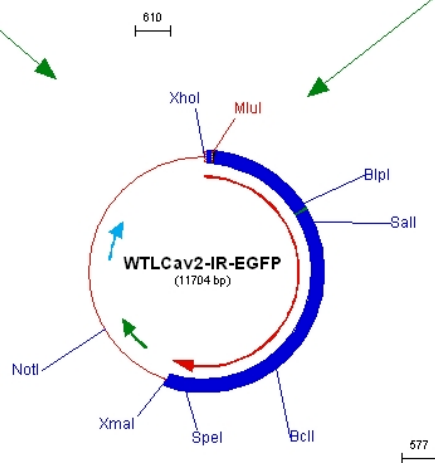


Figure 7: Restriction Digestion Map of WT*LCa_v2*-IR-EGFP, the final plasmid containing wild type *LCav2* gene in pIRES2-EGFP vector. Lane M is 1 kb plus DNA ladder, with 3 brightest bands of 5kb, 1.5kb and 500bp respectively. Lane 1 is blank; lane 2 and lane 3 are both 1µg plasmid DNA of construct digested by BglII, displaying multiple bands of 5480bp, 2842bp, 2335bp, 660bp, 366bp and 21bp (unseen) as expected; lane 4 is 1µg plasmid DNA digested by HindIII, displaying multiple bands of 5289bp, 3359bp and 2956bp as expected. Lane 5 is 1µg uncut plasmid DNA. DNA samples were electrophoresed on 1% TAE agarose gel.

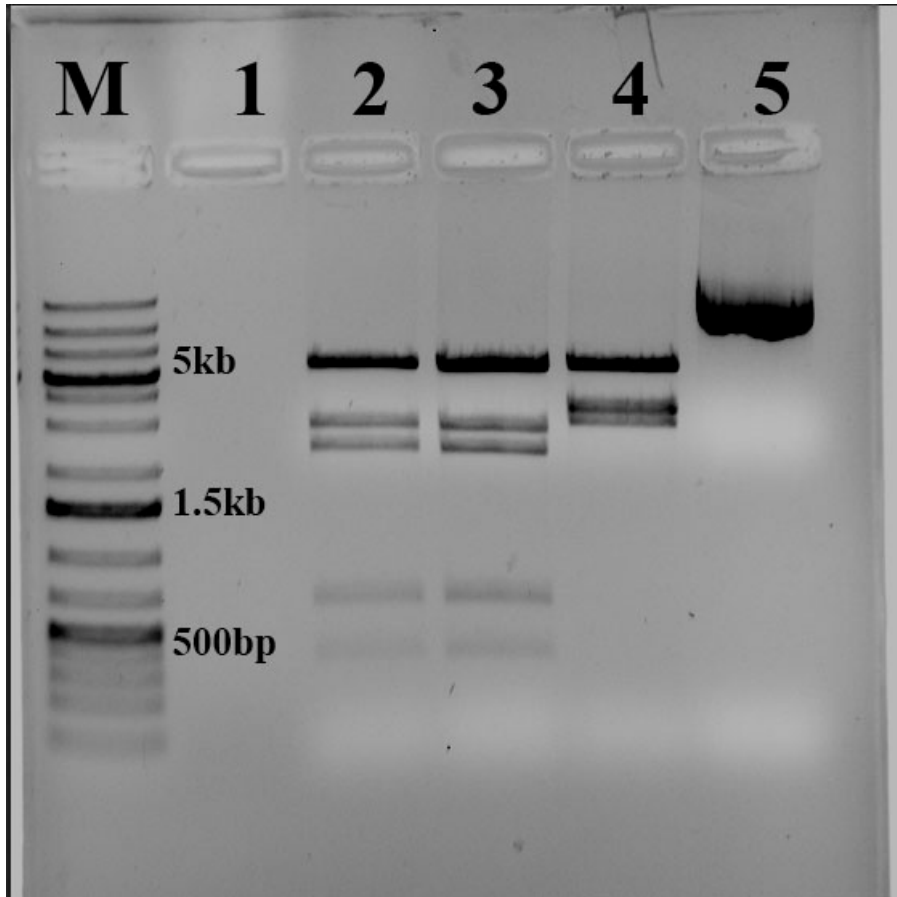


Figure 8: Immunostaining of LCa_v2 transfected HEK-293T cells. After fixation, cells were incubated with 1:1000 chicken anti- LCa_v2 antibody which recognizes a cytoplasmic epitope coding for KAEDNENDSEQNDND. Anti- LCa_v2 antibody was visualized with fluorescently-coupled AlexaFluor633 dye conjugated Goat anti-chicken secondary antibodies. Panel A indicates green fluorescence of the EGFP expressed from $WTLCa_v2$ -IR-EGFP plasmid; panel B indicates AlexaFluor 633 fluorescence of secondary antibody; panel C is Differential Interference Contrast (DIC) image under a Zeiss 510 Meta confocal microscope and panel D is the merged image of fluorescence and DIC (Adriano unpublished data, 2007).

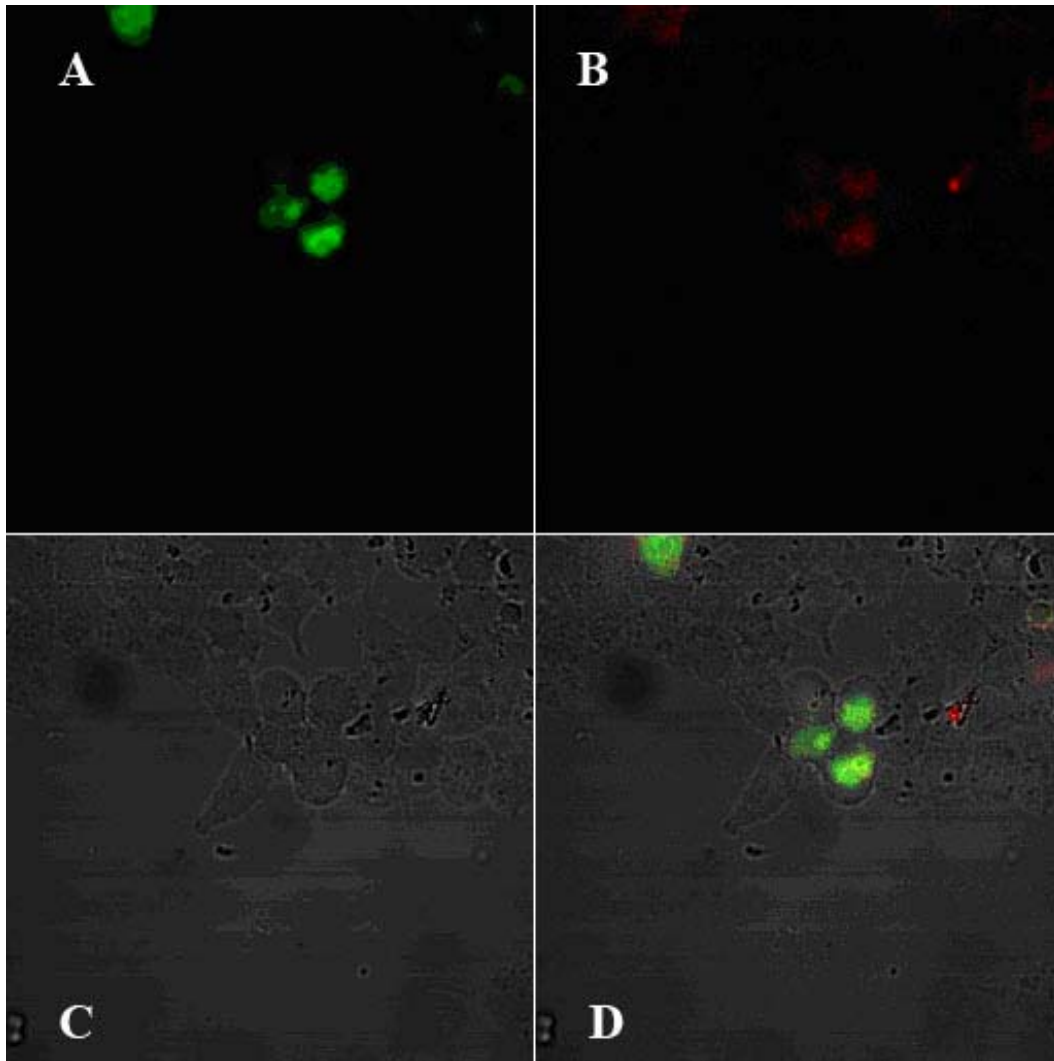


Figure 9: Sample trace of $L\text{Ca}_v2$ barium current. The top panel shows the commanded voltage, consisting of a +20mV step depolarization lasting for 450ms from an initial holding potential at -100mV. The panel at the bottom shows the corresponding current elicited by the voltage step. An inward current as large as 227pA was generated by the +20mV step depolarization.

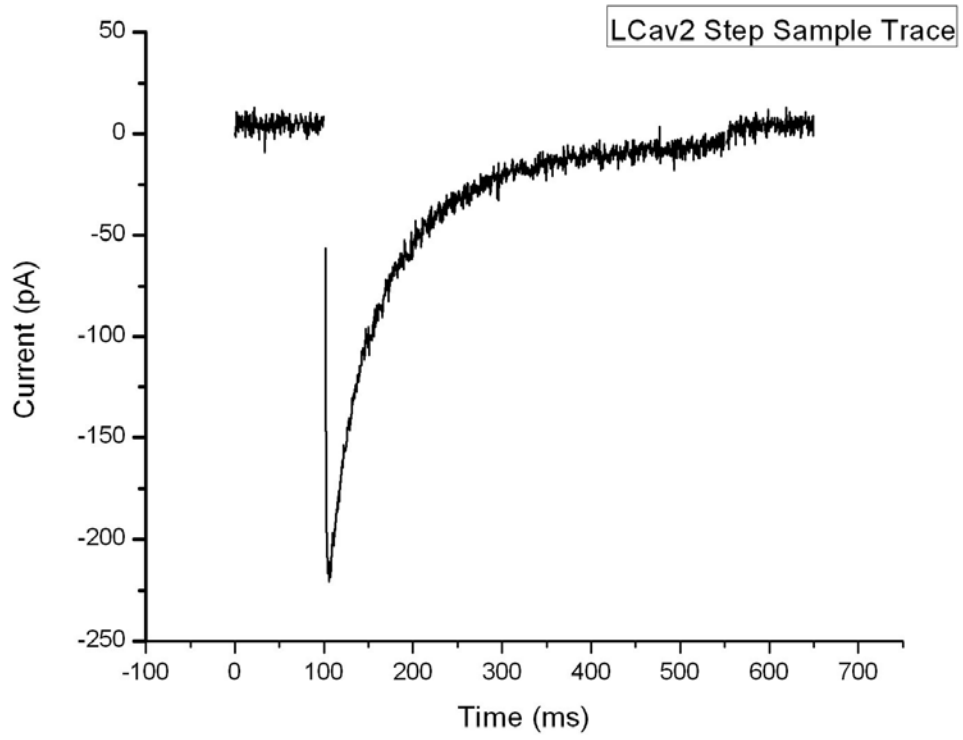
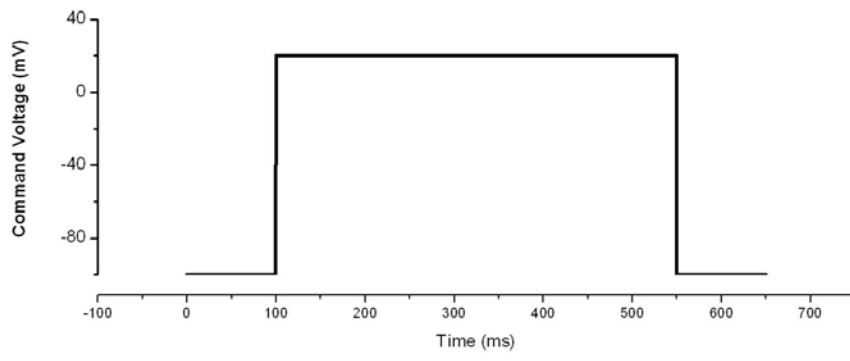


Figure 10: Sample ensemble current traces of LCa_v2 (bottom trace) elicited by voltage steps (top trace) when barium was the charge carrier. Currents were generated by 150 ms testing potentials stepped to -50mV to +60mV at 10mV intervals, from a holding potential at -100 mV.

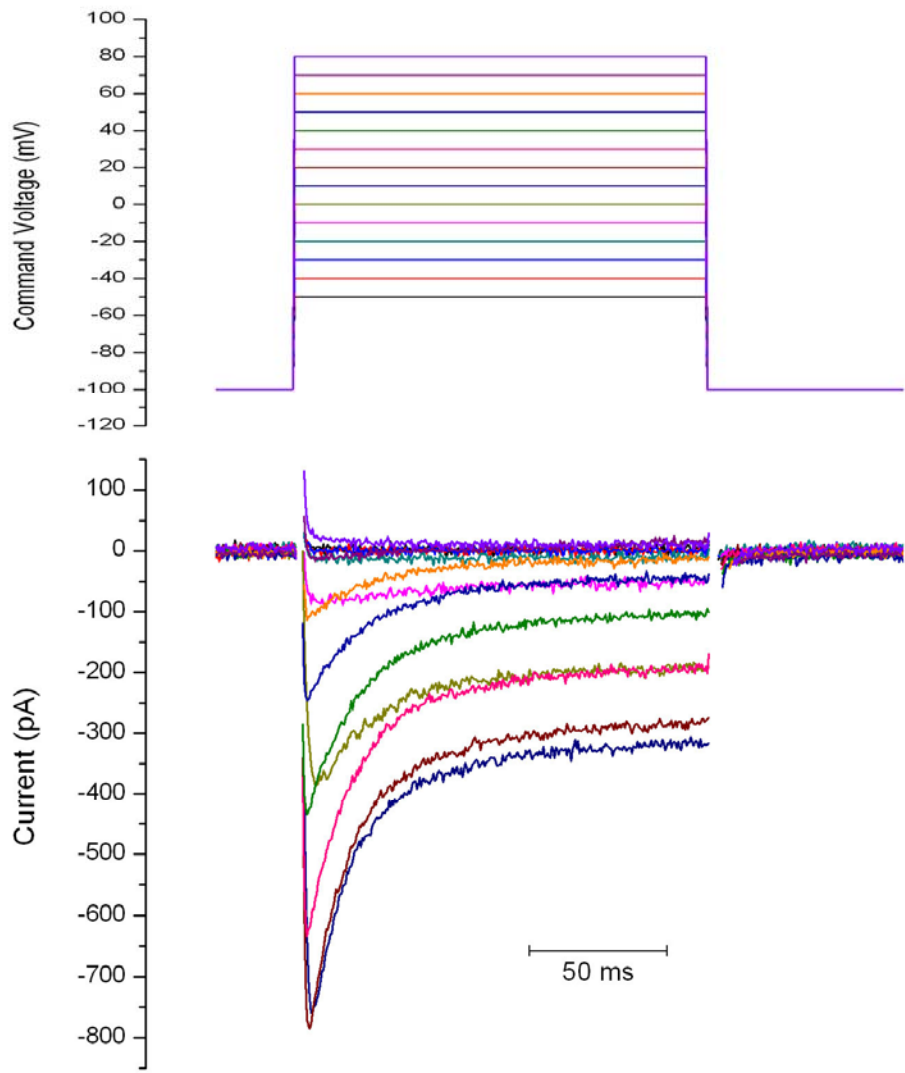


Figure 11: Current-voltage relationship comparisons of LCa_v2 and $rCa_v2.2$ calcium channel homologs. Under identical conditions (20mM barium contained in extracellular solution), both $LCav2$ and $rCav2.2$ started to activate at -20mV and reached the maximal current values at approximate +20mV. Data from seven LCa_v2 transfected and six $rCa_v2.2$ transfected cells were illustrated as mean \pm standard error. Numbers in the figure are replicate numbers.

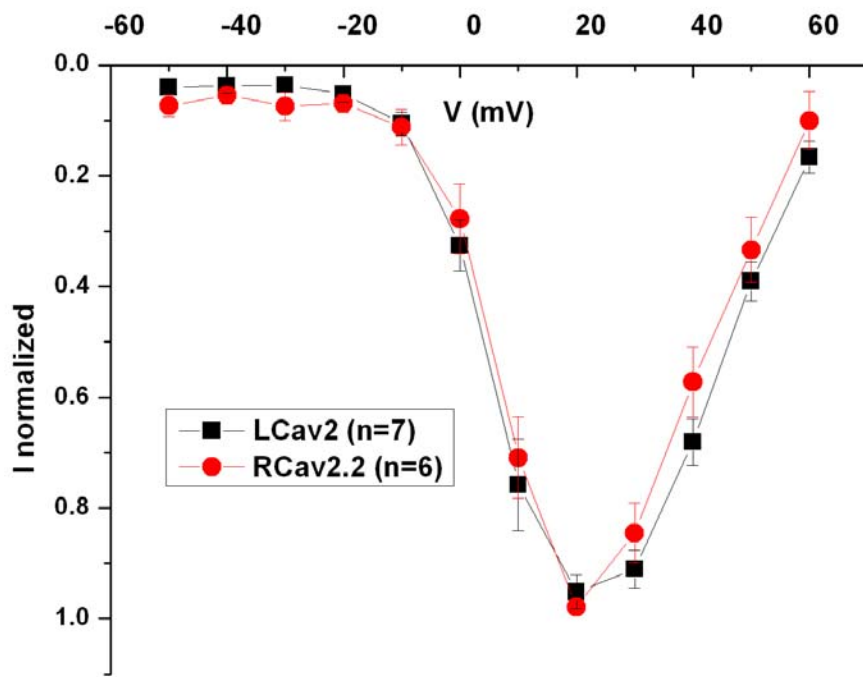


Figure 12: Comparisons of the inactivation decay. Hold at -100mV, membrane potential stepped to +20mV for 450mS. Barium currents through Ca_v2 calcium channel homologs, LCa_v2 and $rCa_v2.2$ were elicited. Normalized mean values of current data at each time point from seven LCa_v2 and eight $rCa_v2.2$ cells were shown. Tau values for inactivation decay were calculated by exponential fitting and were 43.2 ± 1.22 ms and 130.6 ± 0.85 ms for $LCav2$ and $rCav2.2$, respectively. Data were illustrated as mean value \pm standard error. Numbers in the figure are replicate numbers.

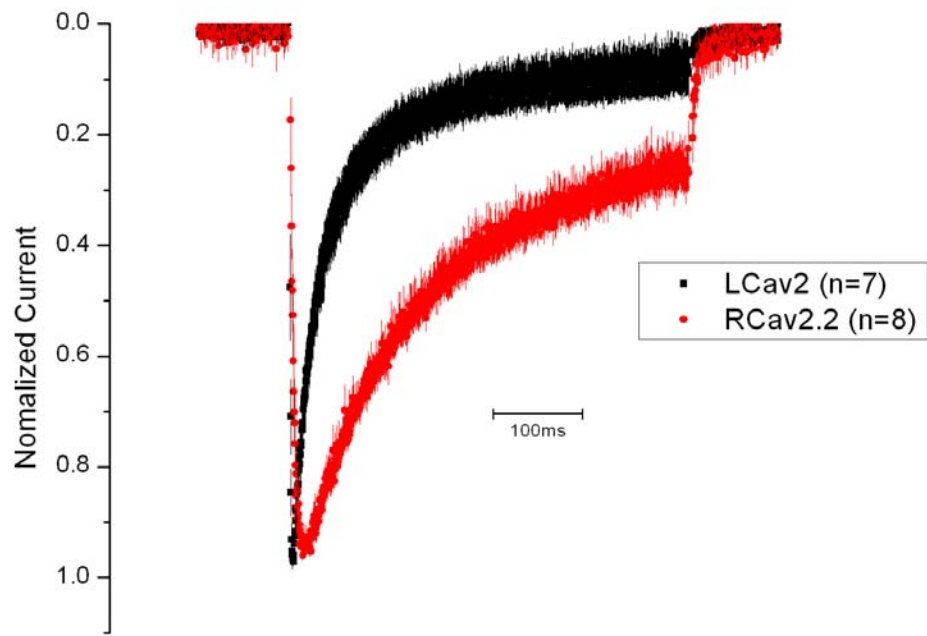
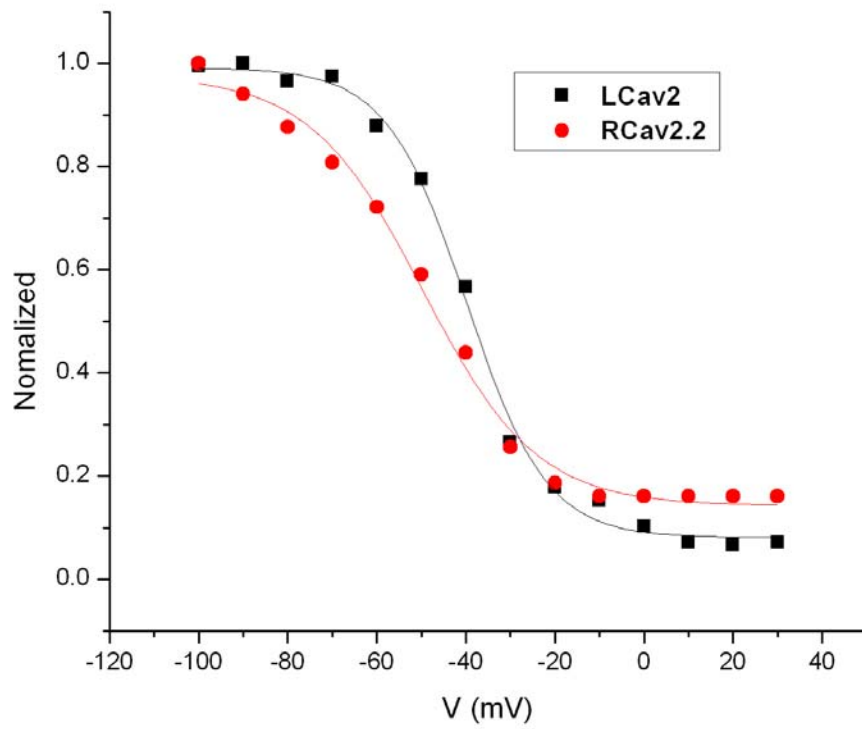
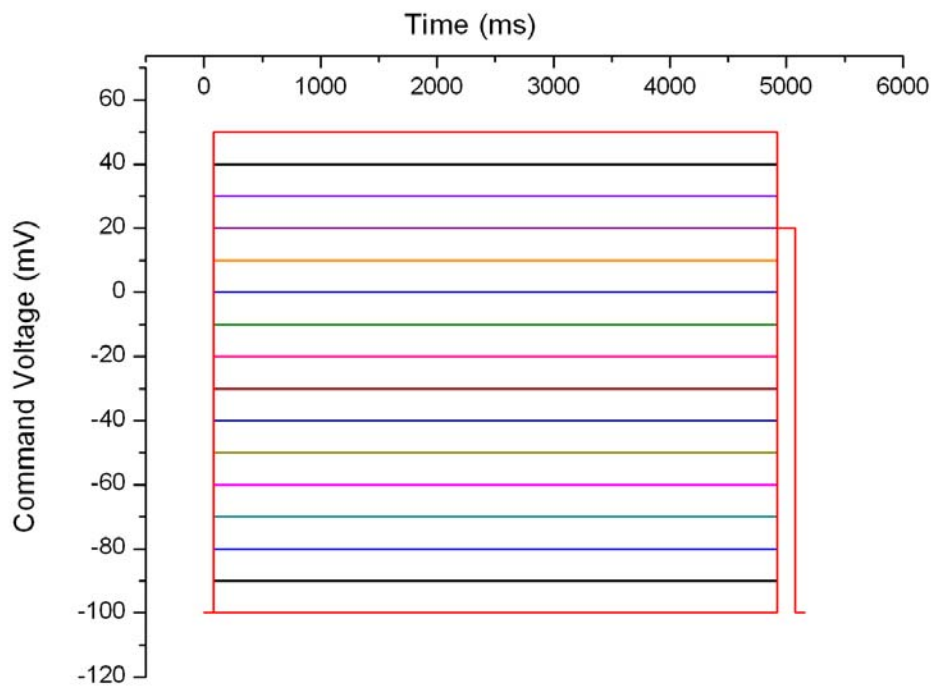


Figure 13: Steady state inactivation curves for LCa_v2 and $rCa_v2.2$ barium currents. A four second depolarizing step was applied to inactivate a fraction of channel activity at different voltages (-90 mV to +70 mV) evaluated by a test pulse at peak current (+20mV for 150 ms). Voltage command protocol (top panel) and steady state inactivation curves are shown. The half-inactivated voltage potential was -39.8 ± 0.82 mV and -49.6 ± 1.45 mV for LCa_v2 and $rCa_v2.2$ respectively.



3.2 *LCa_v2* Calcium Channel Lacks Voltage Dependent G Protein Modulation

Preliminary investigation indicated similarities between *LCa_v2* and *rCa_v2.2* in biophysical characteristics. These channels also play homologous roles in the nervous system as mediators of synaptic transmission. Modulation of synaptic calcium channels by neurotransmitter-gated, G protein coupled receptors is a primary means to alter synaptic efficacy in mammalian synapses, by inhibition of calcium channels. The primary form of G protein regulation in mammals is the voltage-dependent inhibition, which can be relieved by strong depolarizing prepulses. Preliminary investigation of G protein regulation in invertebrates appears to be qualitatively different from the mammalian voltage-dependent G protein modulation: Treatment of *LCa_v2* channels with a non-hydrolysable GTP analog, GTP- γ S leads to constitutive activation of G proteins, and a voltage-independent G protein modulation, where peak currents run down over time without relief of the inhibition by depolarizing prepulses (Spafford et al., 2003b). Depression of presynaptic neurotransmission was by inhibiting calcium currents through a cAMP-mediated G-protein-coupled pathway (McCamphill et al., 2008).

To analyze whether the G protein modulation of *LCa_v2* involved the direct, voltage-dependent inhibition by G protein beta and gamma subunits, 8 μ g *LCa_v2* channels were coexpressed with 2 μ g rat G β ₁ and G γ ₂ subunits per 100 mm culture dish for transfection. Since Current-Voltage relationship of both channels peaked at +20mV, the voltage dependence of G protein modulation was measured by a paired-pulse protocol, by examining the effect of a strong depolarization (+150mV for 50ms) 25 ms before a test pulse (a +20mV step depolarization to +20 mV). A paired-pulse facilitation (PPF) ratio was measured by

comparing the size of the peak current aroused by the test pulse in the presence and absence of the depolarizing prepulse, reflecting the degree of voltage-dependent relief from G protein modulation. If the PPF ratio is significantly above one, which means the peak current with a prepulse is larger than that without a prepulse, a voltage dependent G protein modulation is present. *LCa_v2* currents were unaffected by a strong depolarizing prepulse (Figure 14), compared to *rCa_v2.2*, where the paired-pulse facilitation ratio was significantly larger than one. Data from multiple cells were analyzed (Table 2). In the presence of co-expressed G protein beta gamma subunits, the PPF ratio was 1.95 ± 0.11 , $n=8$ for *rCa_v2.2*. Background endogenous expression of G protein beta gamma subunits in HEK293T cells provides a reduced (1.37 ± 0.07 , $n=9$) but still statistically significant pre-pulse facilitation with *rCa_v2.2*. In comparison, *LCa_v2* channels without or with coexpression of G protein beta gamma subunits, bore a PPF ratio around one (1 ± 0.03 , $n=8$, and 0.95 ± 0.03 , $n=7$, respectively). Statistical analysis using Multiple Turkey Test ($p < 0.05$) revealed relative degrees of PPF were $rCa_{v2.2}/G\beta\gamma > rCa_{v2.2} > LCa_{v2}/G\beta\gamma \sim LCa_{v2}$. The *LCa_v2* ratio was near one reflecting a lack of voltage dependent G protein modulation for *LCa_v2* channels (Figure 15).

The absence of voltage-dependent G protein modulation might be caused by the incompatibility of the rat G protein beta subunit with the snail calcium channel. *Lymnaea* G protein beta1 bears protein identity of 83.9%, 83.6%, 79.8% and 81.8% with rat G protein beta1 through beta4 respectively. The only G protein beta subunit that contributes very little G protein modulation, G protein beta 5 (Arnot et al., 2000; Doering et al., 2004) is more distant to *Lymnaea* G protein beta1 with a gene identity of 50.7%. Even with coexpression of *Lymnaea* G beta1 instead of rat G beta1, voltage-dependent G protein modulation of *LCa_v2*

channels was still evidently lacking, since the paired-pulse facilitation ratios were near unity (1.02 ± 0.117 , $n=2$) (figure 16). Interestingly, coexpression of *rCa_v2.2* with *Lymnaea* G protein beta subunits, did not significantly alter the PPF ratio compared to endogenous G protein modulation (1.33 ± 0.1 , $n=3$) (figure 16). The apparent absence of contribution of *Lymnaea* G protein beta subunits to pre-pulse facilitation of *Ca_v2.2* channels indicated that the G protein beta subunit as well as the *Cav2* calcium channel in *Lymnaea* lacked the structural elements for voltage-dependent G protein modulation.

Figure 14: Sample trace of pre-pulse facilitation of LCa_v2 and $rCa_v2.2$ with the exogenous expression of rat $G\beta 1\gamma 2$ subunits. With a prepulse (150 mV for 50ms in duration, 25ms preceding the test pulse), the peak current of LCa_v2 did not change while the peak current of $rCa_v2.2$ was almost twice as large as the original value. Picture inset illustrates the pre-pulse facilitation protocol.

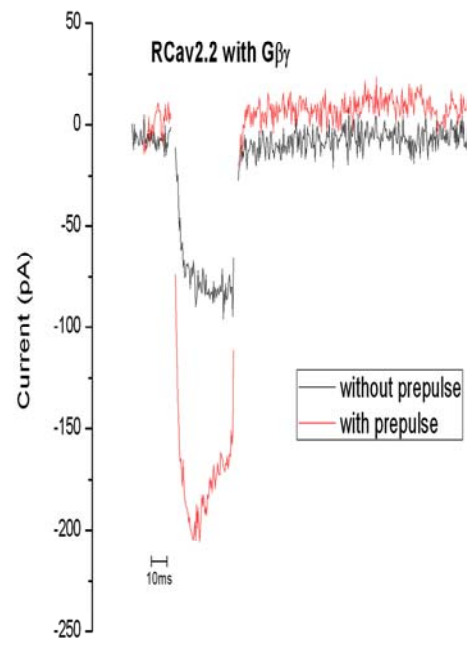
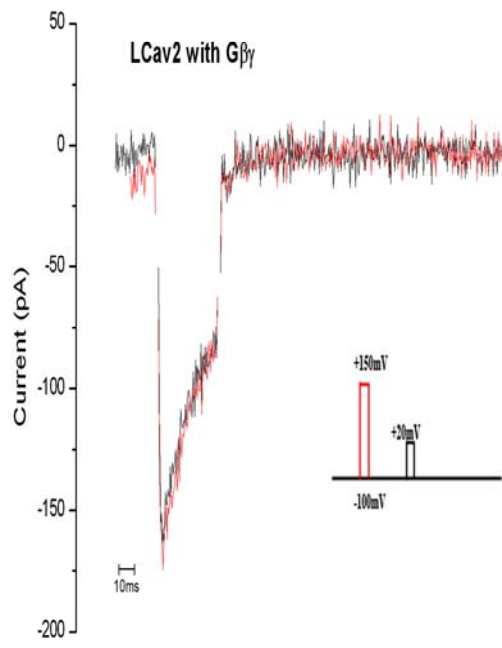


Table 2: Paired-Pulse Facilitation (PPF) ratios describing the voltage dependent G protein modulation of Ca_v2 channels, LCa_v2 or $rCa_v2.2$ in the presence and absence of co-expressed, exogenous rat $G\beta\gamma$ subunits. All the data points used for Figure 15 are provided in the table below.

<i>LCav2</i>	0.9535	1.1853	1.0055	0.9829	1.0413	0.9543	0.8694	0.9902	
<i>LCav2/Gβγ</i>	1.0422	0.8039	0.8704	0.9720	1.0326	0.9269	1.0052		
<i>rCav2.2</i>	1.6604	1.4959	1.0798	1.2127	1.2259	1.1473	1.5574	1.4863	1.4528
<i>rCav2.2/Gβγ</i>	2.0709	2.1150	1.3426	2.2203	1.9444	1.8465	2.3015	1.7275	

Figure 15: Histogram summarizing the paired-pulse facilitation (PPF) of invertebrate LCa_v2 and mammalian $rCa_v2.2$ calcium channels. Columns were illustrated as mean \pm SE. The ratios of the amounts of transfected subunits were: $Ca_v\alpha1: Ca_v\beta: Ca_v\alpha2\delta: rG\beta: rG\gamma = 4: 3: 3: 1: 1$. The PPF ratios for LCa_v2 and $rCa_v2.2$ alone were 1 ± 0.03 (n=8) and 1.37 ± 0.07 (n=9). With the coexpression of Rat $G\beta_1\gamma_2$, the PPF ratio were 0.95 ± 0.03 (n=7) and 1.95 ± 0.11 (n=8) respectively. The PPF ratios were larger than one for $rCa_v2.2$ indicated that $rCa_v2.2$ channels had voltage-dependent relief of G protein inhibition from a depolarizing pre-pulse while PPF ratios were near unity for LCa_v2 indicating an absence of voltage-dependent G protein modulation. Numbers in the figure are replicate numbers.

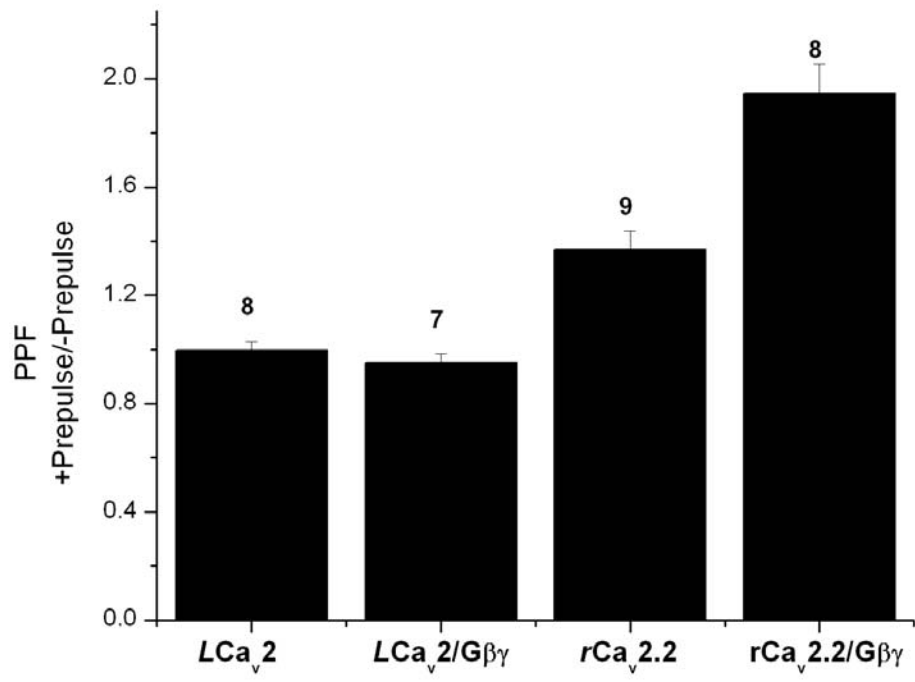
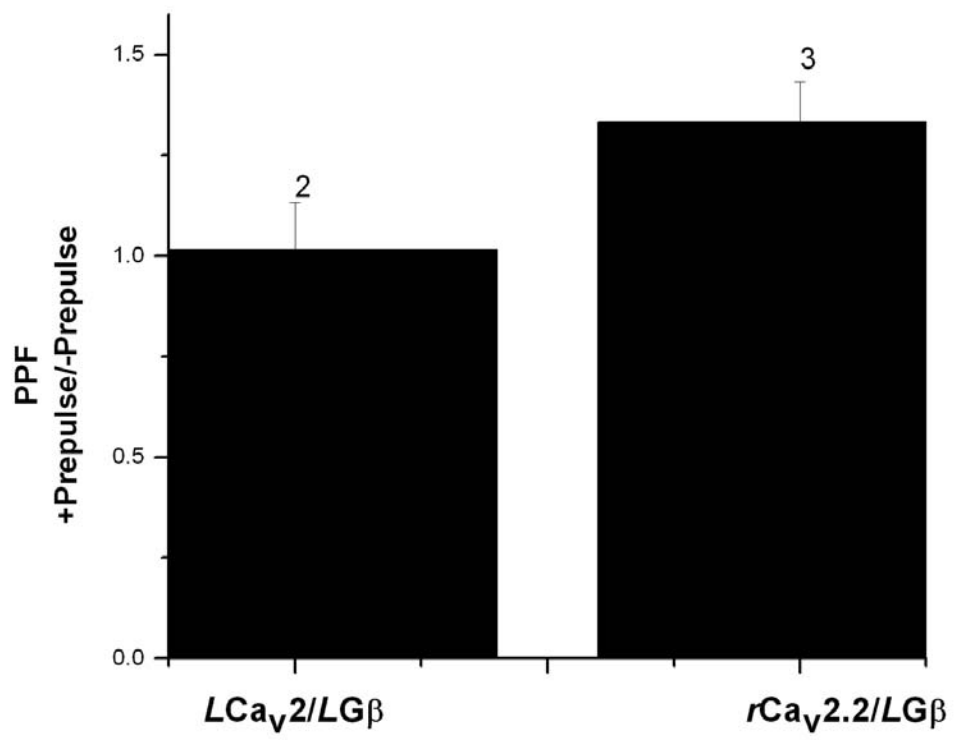


Figure 16: Histogram illustrating the paired-pulse facilitation of mammalian $rCa_v2.2$ and invertebrate LCa_v2 channels coexpressed with invertebrate G protein beta subunit $LG\beta_1$. Columns are shown as mean values with SE error bars. The paired pulse facilitation ratios for LCa_v2 and $rCa_v2.2$ were 1.02 ± 0.117 (n=2) and 1.33 ± 0.1 (n=3) respectively. The PPF values for both LCa_v2 and $rCa_v2.2$ with *Lymnaea* G protein beta1 subunit were not different from data collected from calcium channels without exogenous G protein subunits co-expression. These data suggested that the *Lymnaea* G protein beta1 subunit might not be structurally compatible with voltage-dependent G protein modulation. Numbers in the figure are replicate numbers.



3.3 Calcium channel structures responsible for voltage-dependent G protein modulation

Voltage dependent G protein modulation of Ca_v2 calcium channels is reported to be mediated through interaction between Gβγ subunits and the α1 subunit of either vertebrate Ca_v2.1 and Ca_v2.2 α1 calcium channels (Tedford and Zamponi, 2006). The major site of interaction is two consensus binding sites in the cytoplasmic linker between Domains I and II (I-II linker region) of Ca_v2.1 and Ca_v2.2 channels. A recent report suggested that the N-terminus of Ca_v2 channels might also interact with the I-II linker and were essential for the G protein modulatory effect (Agler et al., 2005). Sequence alignment between *rCa_v2.2* and *LCa_v2* indicates discrepancies in the N-terminal and I-II cytoplasmic linker regions (Figure 17). To explore which structure module is vital for voltage dependent G protein modulation, we tried to swap the I-II linker and the N-terminus from *rCa_v2.2* into *LCa_v2*, attempting to confer voltage dependent G protein modulation to *LCa_v2* which bears prominent voltage-independent G protein modulation, but not voltage-dependent one. The I-II linker and N-terminus chimeras were named _L1_R2_L3_L4 and _R1_L2_L3_L4 respectively, with the Arabic number symbols 1, 2, 3 and 4 representing the four repeated transmembrane domains, the letter L representing the cytoplasmic connecting regions from invertebrate *LCa_v2* channel and the letter R representing the cytoplasmic connecting regions from mammalian *rCa_v2.2* channel.

3.3.1 Construction of the *LCa_v2* chimera with a mammalian I-II linker (_L1_R2_L3_L4) or mammalian N-terminus (_R1_L2_L3_L4)

The chimeric *LCa_v2* channels with the I-II linker (_L1_R2_L3_L4) or N-terminus (_R1_L2_L3_L4)

from *rCa_v2.2* were constructed as followed (Figure 18): Step 1, a 2.5 kb MluI-NheI fragment from *WTLCa_v2-IR-EGFP* was cut and ligated into pGEMT (MluI/SpeI) to create mutagenesis shuttle vector, *LCa_v2MSN-pGEMT* (MluI-SpeI/NheI). For this cloning, NheI and SpeI were ligated together utilizing their compatible ends; Step 2, Silent restriction sites were constructed in *LCa_v2* delimiting both ends of the I-II linker to facilitate the swapping of the I-II linker from *rCa_v2.2* into *LCa_v2MSN-pGEMT*. At the 5' end of the I-II linker was placed a BamHI restriction enzyme site and a SpeI restriction enzyme site was placed at the 3' end. This included the alteration from GGATCG to GGATCC resulting in a silent mutation in a Serine base (TCG→TCC) and creating a BamHI restriction site. The alteration from ACTTGT to ACTAGT resulted in a silent mutation coding for a Leucine residue (CTT→CTA) and creating an SpeI restriction site. Swapping the N-terminus of *rCa_v2.2* into *LCa_v2MSN-pGEMT* also involved creating unique restriction sites delimiting the 3' end of the N-terminus. This included the alteration from TTC GAG to TTC GAA, resulting in a silent mutation in a Glutamic Acid base (GAG→GAA) and creating a unique SfuI (isochizomer BstBI) restriction site. SfuI (BstBI), BamHI, and SpeI sites were created by QuikChange Mutagenesis PCR (Forward, Primer 3#, Mega with Sfu1; Backward, Primer 4#, Mega with Sfu1 AS; Forward, Primer 5#, Mega with BamHI; Backward, Primer 6#, Mega with BamHI AS; Forward, Primer 7#, Mega with Spe1; Backward, Primer 8#, Mega with Spe1 AS), resulting in mutant plasmids MSN-SfuI and MSN-BamHI-SpeI (Figure 19; Figure 20). A MluI-HindIII fragment from MSN-SfuI, and HindIII-AvrII fragment from MSN-BamHI-SpeI were reinserted into *LCa_v2MSN-pGEMT*, to construct the shuttle vector *LCa_v2SBS-pGEMT*, which contained all three newly synthesized restriction sites, SfuI,

BamHI and SpeI (Figure 21); Step 3, the I-II linker from *rCa_v2.2* was created with compatible 5' BamHI and 3' SpeI restriction site ends in the PCR (Forward, Primer 9#, Ra1b BamH1f; Backward, Primer 10#, Ra1b Spe1b) using *RatCa_v2.2*-pMT2 containing the whole length *rCa_v2.2* sequence in pMT2 vector as the template in the PCR. The I-II linker from *rCa_v2.2* was swapped in place of the I-II linker of *LCa_v2* with BamHI and SpeI restriction enzymes into *LCa_v2*SBS-pGEMT, forming RatLinker-MSN; Step 4, The final *LCa_v2* (_{L1R2L3L4}) chimera (*LCa_v2*(Rat I-II linker)-IR-EGFP) was finished by swapping the mutagenized RatLinker-MSN clone into *WTLCa_v2*-IR-EGFP using MluI and BlnI restriction enzyme sites (Figure 22).

The N-terminus of *rCa_v2.2* was also cloned into the shuttle vector *LCa_v2*SBS-pGEMT. However, due to the high GC content and repeated sequences in this region, attempts to amplify the NT of *rCa_v2.2* in the PCR failed several times, producing sequences with multiple deletions. A cloning strategy was applied using opportunistic restriction sites instead (Figure 23). Generally, two steps were involved in creating the N terminus chimera: first, the N terminal region of *rCa_v2.2* including a CMV promoter in the vector was cut from *Rata1b*-pMT2 and inserted to the shuttle vector *LCa_v2*SBS-pGEMT resulting in the RatNT-MSN, where the N-terminus of *LCa_v2* was interrupted and replaced. Then, the final N-terminus chimera *LCa_v2*(_{R1L2L3L4}) (*LCa_v2*(RatNT)-IR-EGFP) was finished by swapping the mutagenized RatNT-MSN clone into *WTLCa_v2*-IR-EGFP using MluI and Sall restriction enzyme sites. This final plasmid was confirmed by double digestion (Figure 24).

3.3.2 *LCa_v2* (_{L1R2L3L4}) and *LCa_v2* (_{R1L2L3L4}) chimeras lack the property of voltage

dependent G protein modulation

4 μ g *LCa_v2* (_L1_R2_L3_L4) or *LCa_v2* (_L1_R2_L3_L4) chimera were cotransfected with 3 μ g *rβ₁* (pMT2), 3 μ g *rα2-δ* (pMT2) and 1 μ g of rat G protein β₁γ₂ subunits into HEK293T cells and tested for relief of inhibition by G proteins using the paired-pulse facilitation protocol. It has been reported that the cytoplasmic I-II linker and N-terminus are necessary to confer voltage-dependent G protein modulation (De Waard et al., 1997), while our data suggested that these two regions operating alone is not enough to confer the voltage dependent property to *LCa_v2* channel. As illustrated in figure 25, under the endogenous G protein modulation from background G proteins in HEK cells, the PPF ratio value for *LCa_v2* (_L1_R2_L3_L4) was 0.94 ± 0.01 (n=2); with the exogenous G protein modulation over the background, the PPF ratio values for *LCa_v2* (_L1_R2_L3_L4) and *LCa_v2* (_L1_R2_L3_L4) were also near the unity: 0.90 ± 0.04 (n=5) and 0.89 ± 0.05 (n=2) respectively.

Figure 17: Amino acids sequence alignment of N-terminus and I-II linker among rat Ca_v2 family ($rCa_v2.1$, 2.2 and 2.3) and LCa_v2 . Identical amino acids are in grey shadows while major discrepancies are in red boxes. Locations of the silent mutations are also indicated: a BamHI (GGATCC) site was designed in a Serine residue by an alteration from TCG to TCC; a SpeI (ACTAGT) site was designed in a Leucine residue by an alteration from CTT to CTA; and a SfuI (isochizomer BstBI) site was designed in a Glutamic Acid (TTC GAA) residue by an alteration from GAG to GAA.

N Terminus Sequence Alignment

<i>LCav2</i> MATFQANNGQQDDGDNTTNQDGPFS	25
<i>rCav2.1</i>	MARFGDEMP - GRYGAGGGGSGPAAGVVVGAAGGRGAGGSRQGGQPGAQR - MYKQSMAQRA	58
<i>rCav2.2</i>	MVRFGDELG - GRYGGTGGGER - - - - - ARGGGAGGAGGPGQGGLPPGQRVLYKQSIQRA	53
<i>rCav2.3</i>	MARFGEAVVVGRPGSGDGDGDS - - - - - DQSRNRQGTVPVPASGPAAAYKQSKAQRA	48

	* *	BstBI(Sful)	ISI
		┌	└
<i>LCav2</i>	HFSRKAALLGLPGMASQST RSLFIFSEENFIRKYAKI IIEWGPFPEYMLLTIIA	79	
<i>rCav2.1</i>	RTMALYNPI PVRQNC LTVNRS LFLFSEDNVVRKYAKKI TEWPPFEYMLATI IA	112	
<i>rCav2.2</i>	RTMALYNPI PVKQNCFTVNRS LFLFSEDNVVRKYAKRI TEWPPFEYMLATI IA	107	
<i>rCav2.3</i>	-TMALYNPI PVRQNCFTVNRS LFI FGEDNIVRKYAKKLIDWPPFEYMLATI IA	101	

I-II Linker Sequence Alignment:

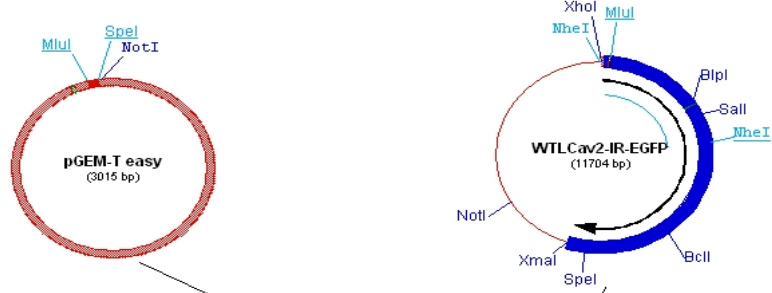
	BamHI	ISI
	┌	└
<i>LCav2</i>	LGSFFMLNLV LGLVLSGEFAKERERVENRRAF F KLRRQQQIERELNGYLEWIC KAAEEVILS	390
<i>rCav2.1</i>	IGSFFMLNLV LGLVLSGEFAKERERVENRRAF L KLRRQQQIERELNGYMEWIS KAAEEVILA	407
<i>rCav2.2</i>	IGSFFMLNLV LGLVLSGEFAKERERVENRRAF L KLRRQQQIERELNGYLEWIF KAAEEVMLA	401
<i>rCav2.3</i>	IGSFFV LNLV LGLVLSGEFAKERERVENRRAF M KLRRQQQIERELNGY R A W I D KAAEEVMLA	396

<i>LCav2</i>	EERTTDEEKLK I EARRQAAARK M QLKAEDNENDSEQNDNDLLAAMAPGNS FKSMKKRR	450
<i>rCav2.1</i>	EDET DVEQRHPFD GALRRAT LKKS KTD LLNPEEAEDQLADIA SVGSPFARAS I KSAKLEN	467
<i>rCav2.2</i>	EEDKNAEEKSP LD - VLKRAAT KKS RND LIH AEEGEDRFVD LCAAGSPFARAS LKSGKTES	460
<i>rCav2.3</i>	EENKNSG - T S A L E - VLRRATI KRS RTEAMTRDSSDEHCVDI S SVGTPLARAS I KSTKVDG	454

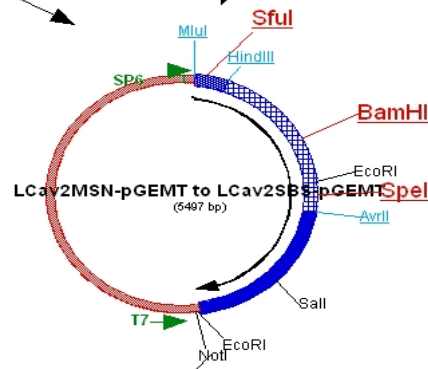
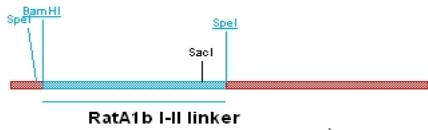
	Spel	IISI
	┌	└
<i>LCav2</i>	TTGKCA S F W R A EKRFRYSIRRLVKSQLFYWIVIVLVF	487
<i>rCav2.1</i>	ST - - - - F F H K K E R R M R F Y I R R M V K T Q A F Y W T V L S L V A	500
<i>rCav2.2</i>	SS - - - - Y F R R K E K M F R F L I R R M V K A Q S F Y W V V L C V V A	493
<i>rCav2.3</i>	AS - - - - Y F R H K E R L L R I S I R H M V K S Q V F Y W I V L S V V A	485

Figure 18: Illustration of Cloning Strategy to Construct LCa_v2 ($L1_R2_L3_L4$) Chimera. Step 1, a 2.5 kb MluI-NheI fragment from $WTLCa_v2$ -IR-EGFP was cut and ligated into pGEMT (MluI/SpeI) to create mutagenesis shuttle vector, LCa_v2 MSN-pGEMT (MluI-SpeI/NheI); Step 2, Silent restriction sites BamHI, SpeI, and SfuI (isochizomer BstBI) were created into LCa_v2 MSN-pGEMT; Step 3, The I-II linker from $rCa_v2.2$ was created in PCR and swapped into LCa_v2 SBS-pGEMT, forming RatLinker-MSN; Step 4, The final LCa_v2 ($L1_R2_L3_L4$) chimera (LCa_v2 (Rat I-II linker)-IR-EGFP) was finished by swapping the mutagenized RatLinker-MSN clone into $WTLCa_v2$ -IR-EGFP using MluI and BlnI restriction enzyme sites. Restriction enzyme sites chosen for cloning are colored blue and underlined. Inserted fragment for each ligation step is marked by a blue line. Silent restriction sites that were created are marked in red. This picture was designed with Gene Construction Kit software (Textco).

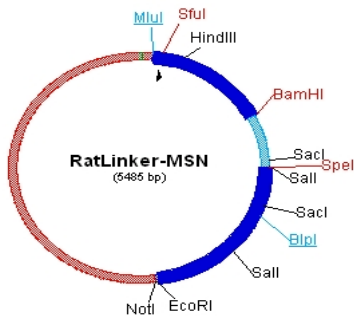
Step 1,
 1, cut WTLcav2 in pIRES2EGFP with Mlu1/Nhe1
 2, cut circulized pGEMT with Mlu1/Spe1
 3, Ligate 2.5kb band of WTLcav2 and 3kb band of pGEM-T
 4, screen by X-Gal and EcoR1 to create LCav2MSN-pGEMT



Step 2,
 1, Quick Change Mutagenesis to introduce Sfu1 site, BamH1 & Spe1 sites respectively;
 2, Cut MSN-Sfu1 WITH Mlu1/HindIII, MSN-BamH1-Spe1 with HindIII/AvrII, to construct LCav2SBS-pGEMT



Step 3,
 1, PCR to get BamH1-RatA1blinke r-Spe1;
 2, ligate to pGEM-T easy;
 3, Cut RatLinker-pGEMT and SBS with BamH1/Spe1 to construct RatLinker-MSN



Step 4,
 Cut RatLinker-MSN and WTLcav2 by Mlu1/Bsp1 to construct RatLinker-Lcav2

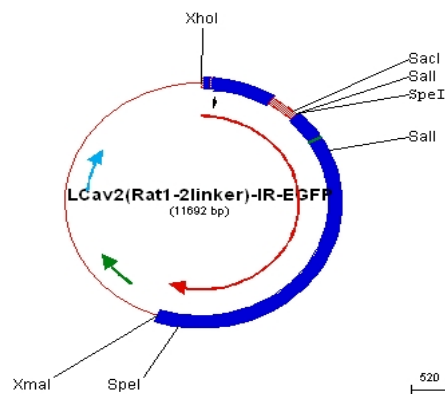
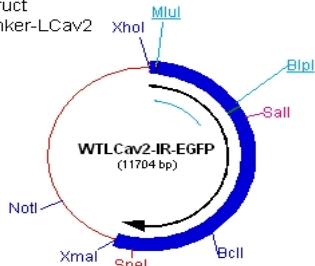


Figure 19: Restriction digestion analyses of three plasmid clones to identify successful SpeI mutants from QuikChange Mutagenesis PCR (Stratagene) to create SpeI restriction sites. Lane M is 1 kb plus DNA ladder, with 3 brightest bands of 5kb, 1.5kb and 500bp respectively. Lane 1, 3, 5 are undigested plasmids while lane 2, 4, 6 are their corresponding digestions by SpeI. Lane 5 and lane 6 represent the clone with the newly created SpeI site in the *LCa_v2MSN-pGEMT* shuttle plasmid, with a single digested band around 5.5kb by SpeI digestion. This mutant clone was confirmed by double digestion and DNA sequencing.

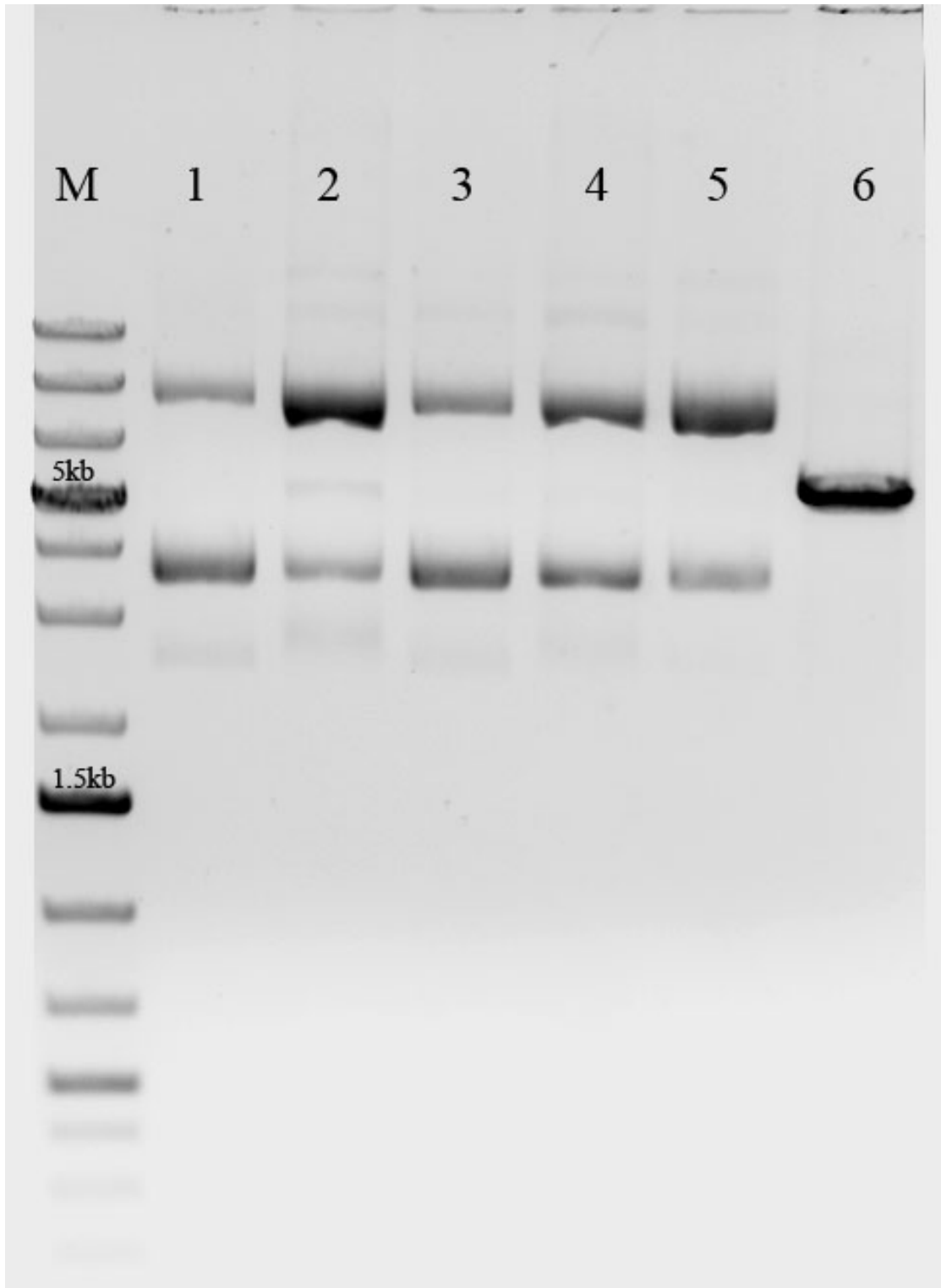


Figure 20: Double digestion to confirm the successful construction of MSN-SfuI, with a newly created SfuI (isochizomer BstBI) restriction site in the *LCa_v2MSN-pGEMT* shuttle plasmid. Lane M is 1 kb plus DNA ladder, with 3 brightest bands of 5kb, 1.5kb and 500bp respectively. Lane 1 is the double digestion by EcoRI and BstBI, with bands of expected sizes 3029bp, 1354bp and 1114bp (indicated by star symbols) while the original *LCa_v2MSN-pGEMT* would result in the digestion pattern of 4143bp and 1354bp (picture not shown).

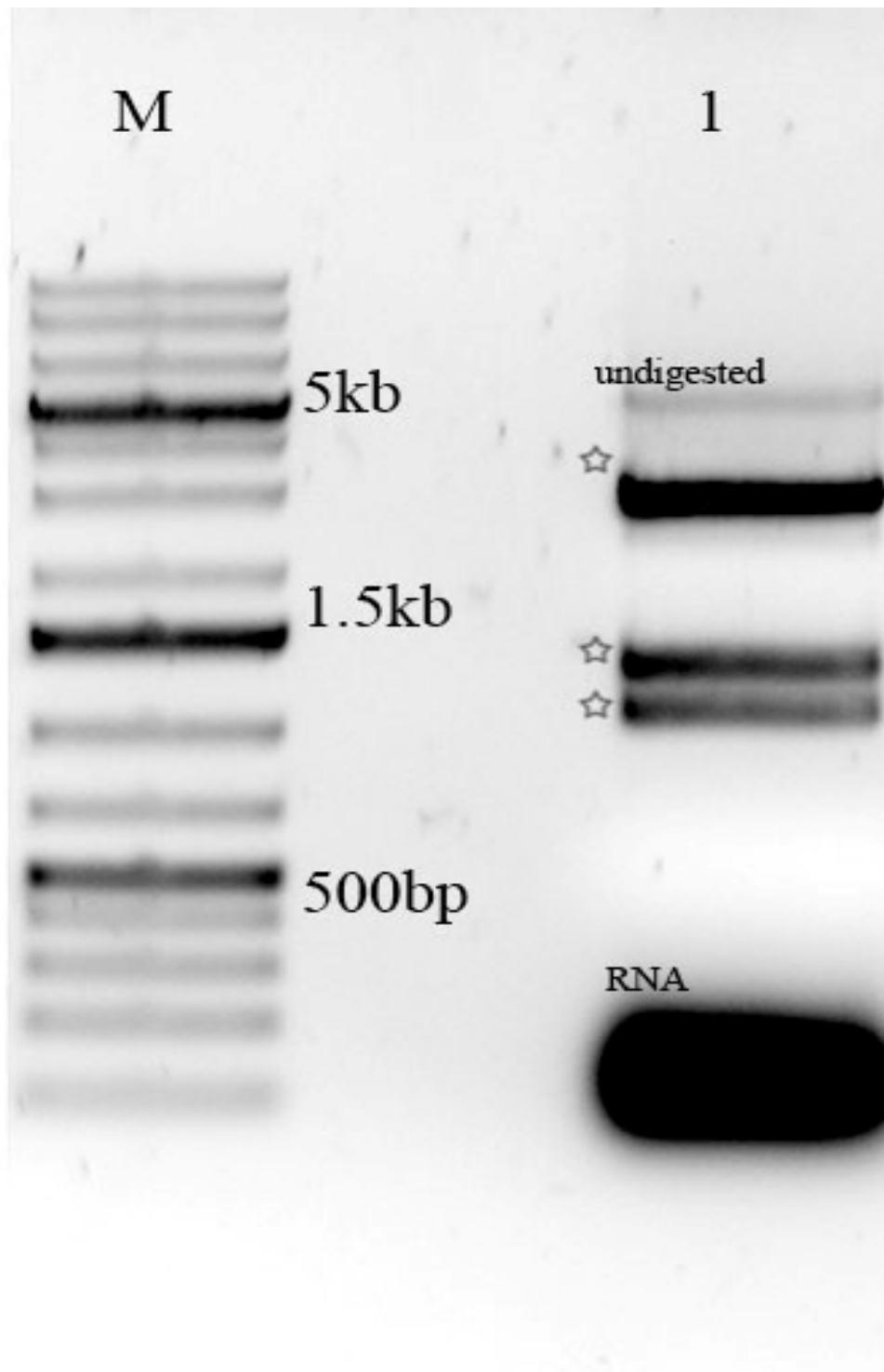


Figure 21: Double digestion to confirm the cloning of shuttle vector *LCa_v2SBS-pGEMT*.

Lane M is 1kb DNA ladder; Lane1 is the uncut plasmid; Lane2 is the double digestion by BamHI/NotI displaying the expected sizes of 3805bp and 1689bp (indicated by star symbols); lane4 is the double digestion by BstbI/SpeI displaying the expected sizes of 4290bp and 1207bp (indicated by star symbols).

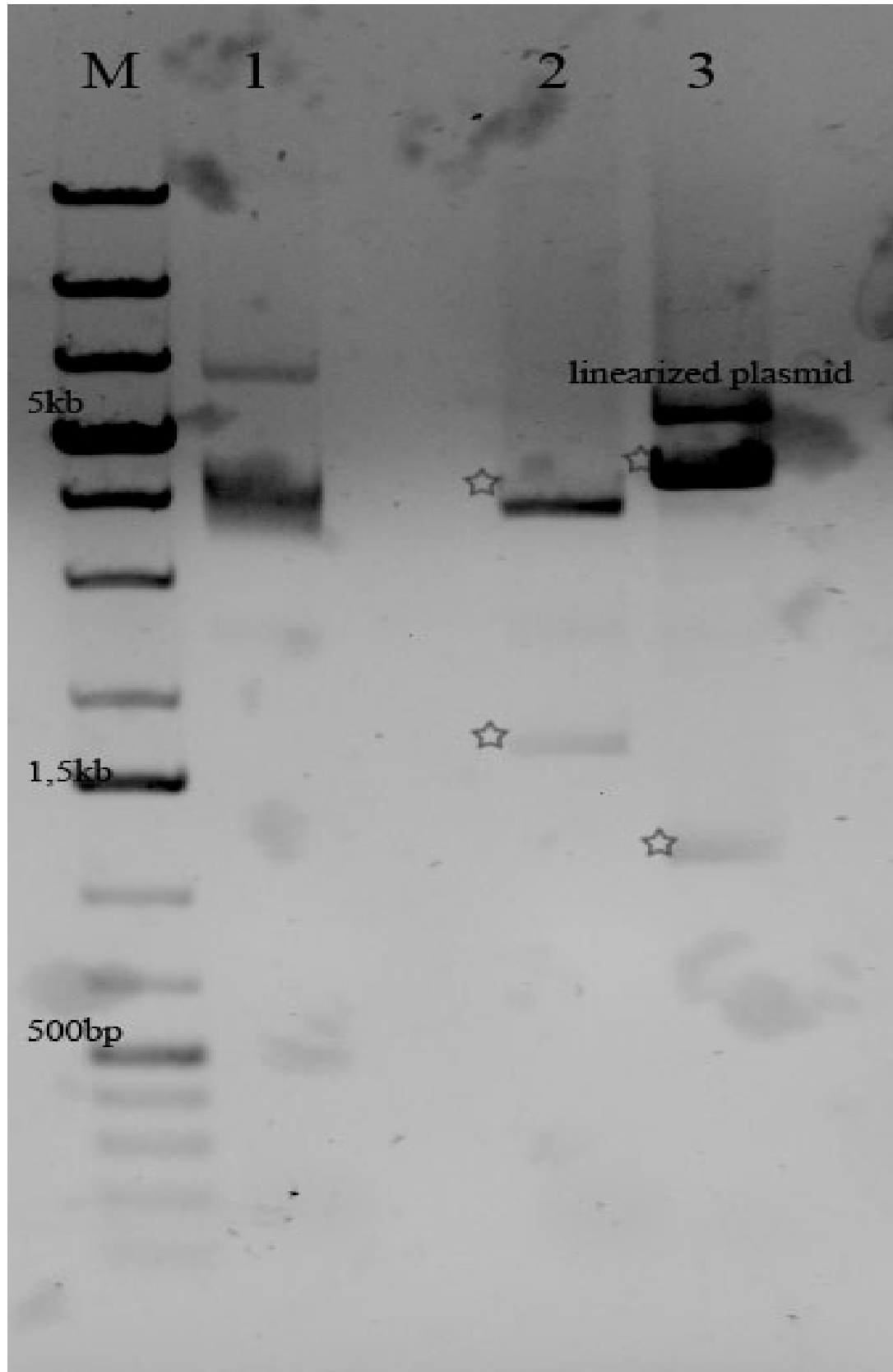


Figure 22: Double digestion to confirm the I-II linker chimera $LCa_v2(L1_R2_L3_L4)$. Lane M is 1kb DNA ladder; lane1 and lane 3 are $WTLCa_v2$ -IR-EGFP digested by SalI and SpeI respectively, which only owns one SalI site and one SpeI site (single bands are indicated by star symbols); lane2 and lane 4 are $LCa_v2(L1_R2_L3_L4)$ chimera digested by SalI or SpeI, which display 10991bp and 701bp pattern, and 7005bp and 4687bp pattern respectively (indicated by star symbols). Note that $LCa_v2(L1_R2_L3_L4)$ plasmid clone contains one extra SalI and SpeI restriction sites, providing two bands after SalI or SpeI digestion instead of one.

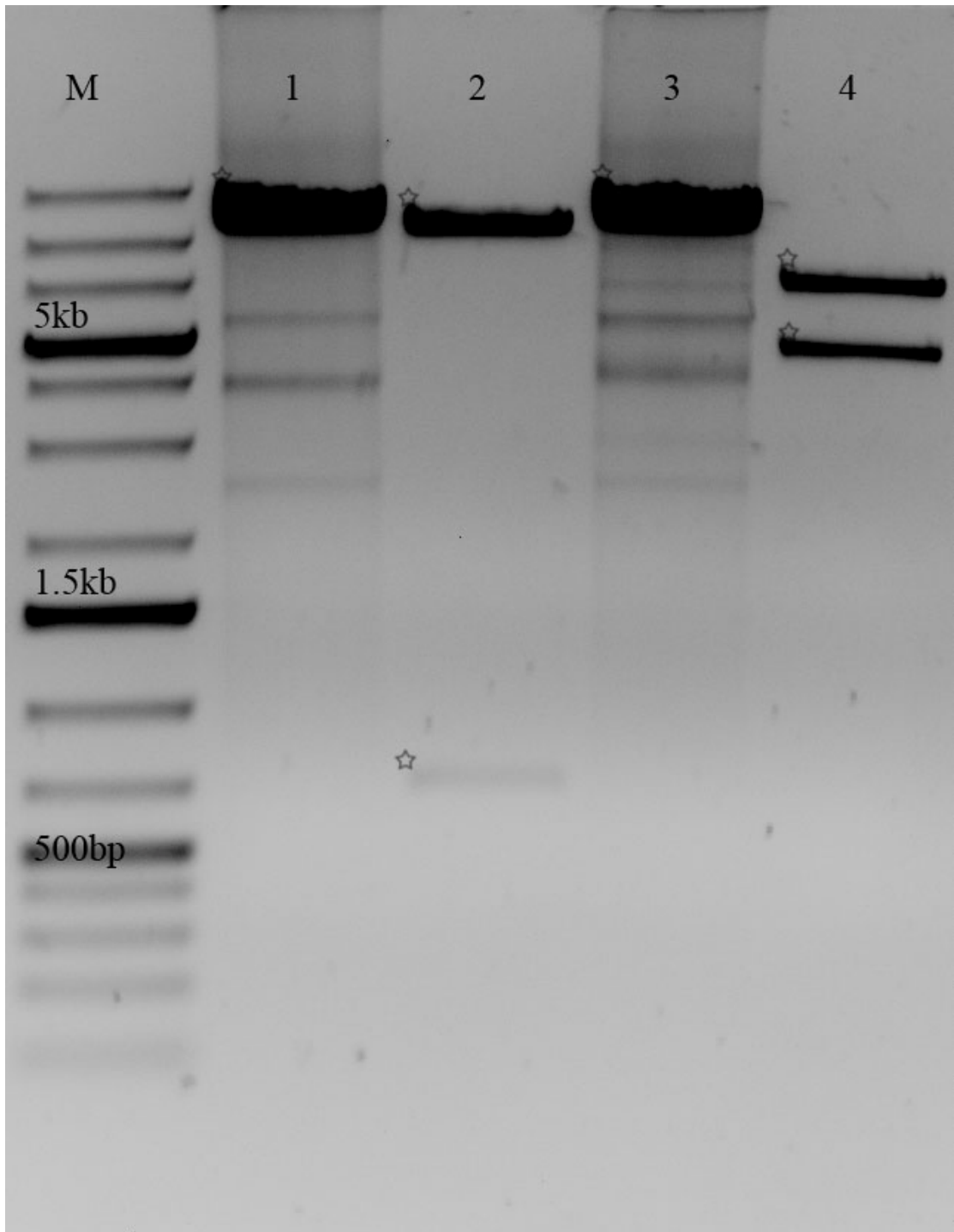
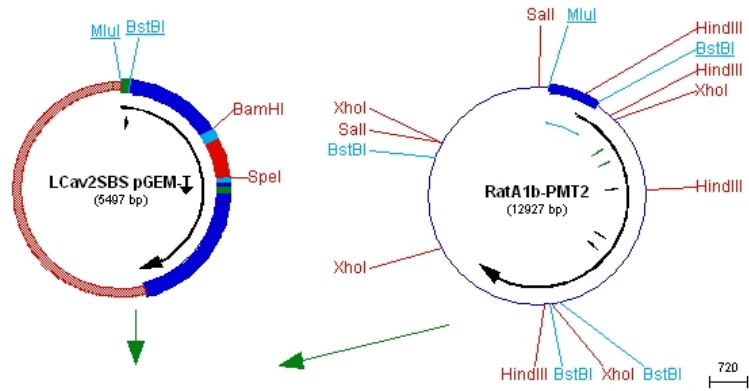
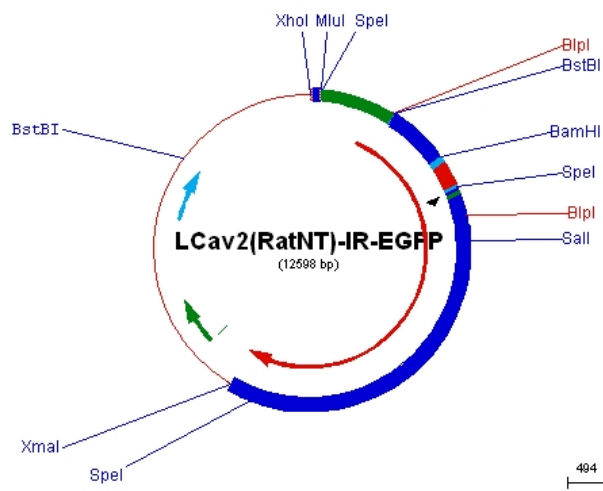
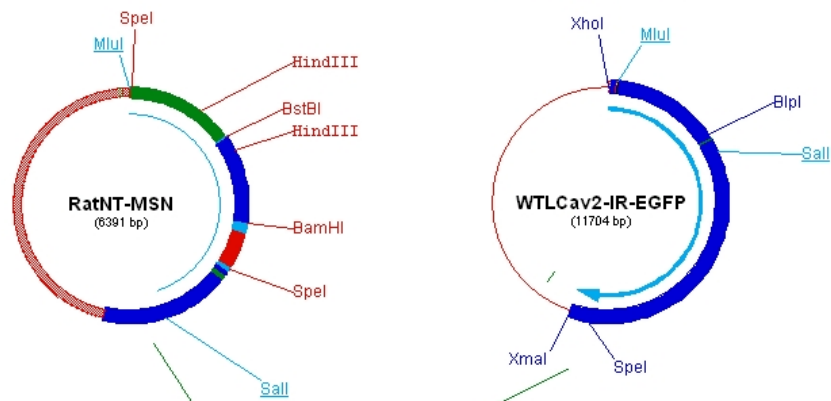


Figure 23: Illustration of Cloning Strategy to Construct $LCa_v2(R1_L2_L3_L4)$ Chimera. Step 1, the N terminal region of $rCa_v2.2$ was inserted to the shuttle vector $LCa_v2SBS-pGEMT$ resulting in the RatNT-MSN; Step 2, the final N-terminus chimera $LCa_v2(R1_L2_L3_L4)$ ($LCa_v2(RatNT)$ -IR-EGFP) was finished by swapping the mutagenized RatNT-MSN clone into $WTLCa_v2$ -IR-EGFP using MluI and Sall restriction enzyme sites. Restriction enzyme sites chosen for cloning are colored blue and underlined. Inserted fragment for each ligation step is marked by a blue line. Silent restriction sites that were created are marked in red. This picture was designed with Gene Construction Kit software (Textco).

Step 1: Cut the shuttle vector LCav2SBS-pGEMT with MluI/BstBI, purify the 5421bp band; Cut RatA1b-pMT2 with MluI/Bstb1, purify the 970bp band; Ligase



Step 2: Cut RatNT-pGEMT with MluI/SalI, purify 2874bp band; Cut WTLCav2 with MluI/SalI, purify the 9741bp band; Ligase



618

Figure 24: Double digestion to confirm the N-terminus chimera $LCa_v2_{(R1L2L3L4)}$. Lane M is 1kb DNA ladder; Lane 1 and lane 2 are the plasmid harboring chimera digested by BspI and NdeI respectively, display 11005bp and 1610bp pattern, and 11838bp and 787bp pattern respectively (indicated by star symbols) while the $WTLCa_v2$ -IR-EGFP bears only one BspI site and one NdeI site.

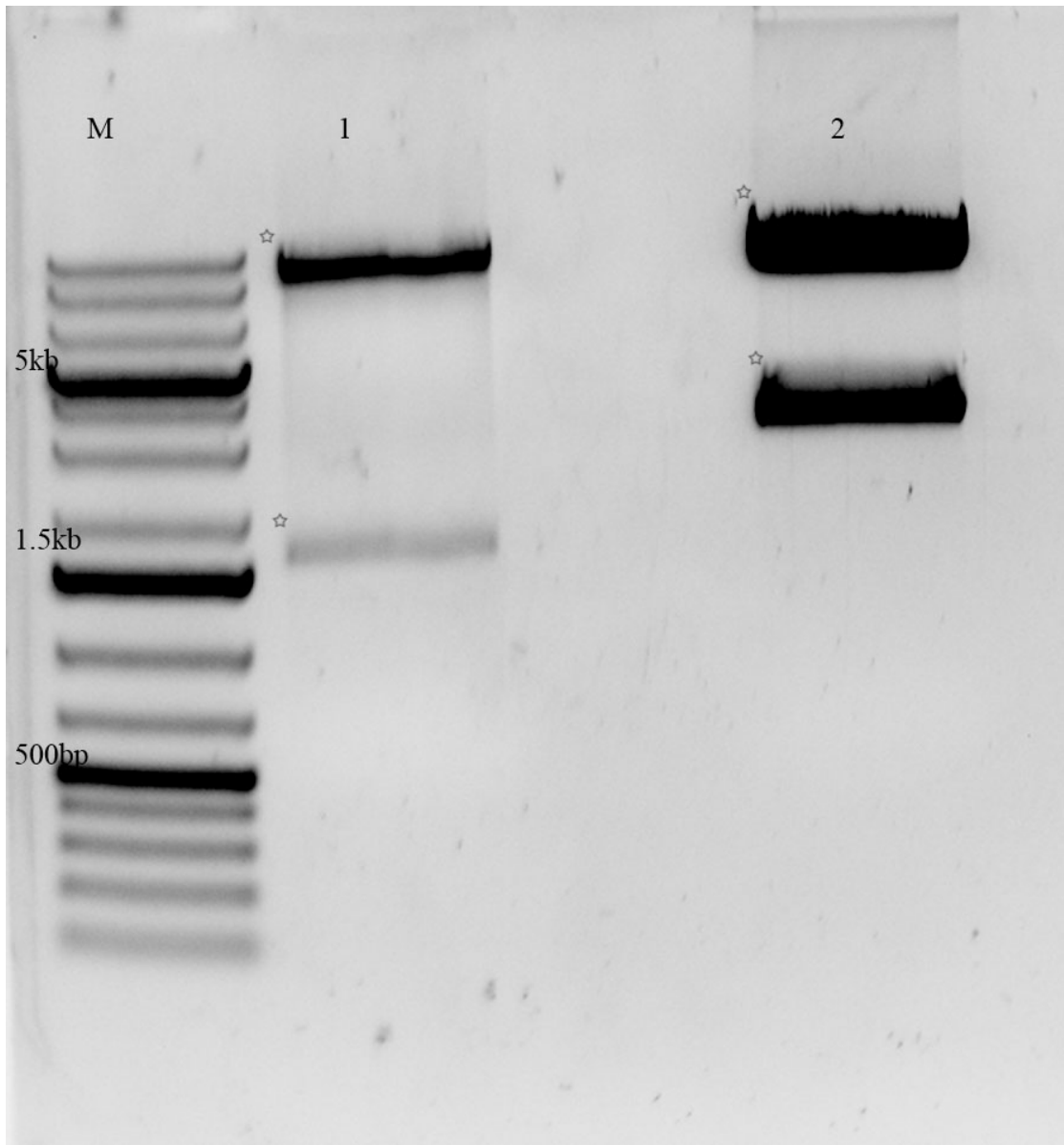
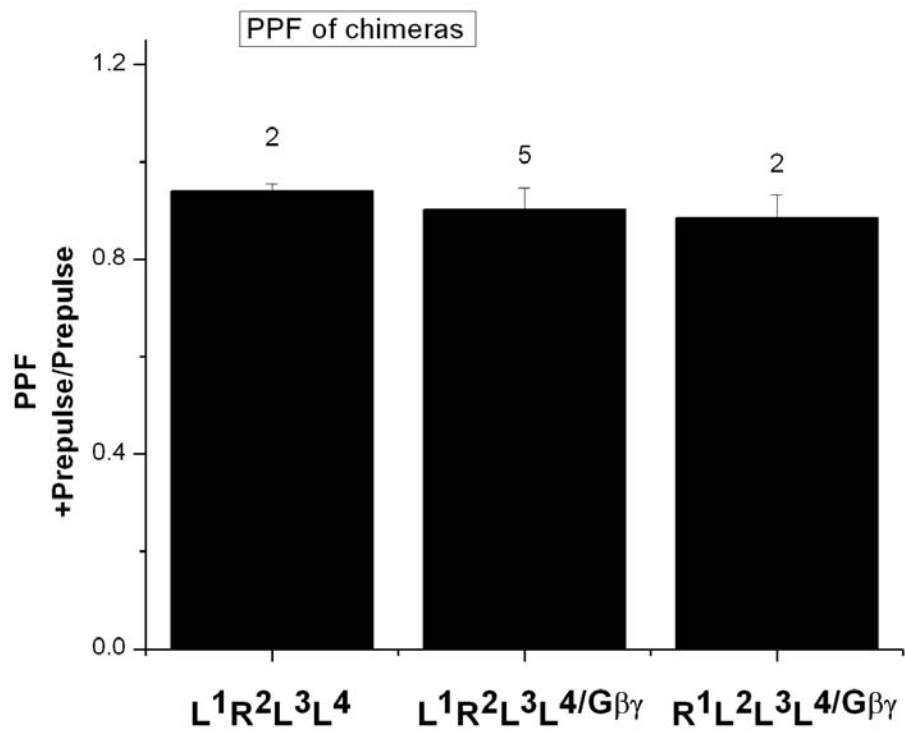


Figure 25: Histogram summarizing the paired-pulse facilitation experiment for I-II linker chimera $LCa_v2(L1_R2_L3_L4)$ and N-terminus chimera $LCa_v2(R1_L2_L3_L4)$. Columns are illustrated as mean values with SE error bars. The PPF ratios for $LCa_v2(L1_R2_L3_L4)$ with endogenous or exogenous mammalian G protein subunits expression are 0.94 ± 0.01 and 0.90 ± 0.04 respectively. PPF ratio for $LCa_v2(R1_L2_L3_L4)$ with exogenous mammalian G protein subunits expression is 0.89 ± 0.05 . Numbers above indicate the amount of replicates. Note that PPF ratios are below unity for these two chimeras, indicating that the mammalian I-II linker or N-terminus alone is not sufficient to generate voltage-dependent G protein modulation in LCa_v2 .



Chapter 4 Discussion

G protein inhibition of presynaptic calcium channels is critical for suppressing synaptic transmission. The timing and strength of neurotransmitter release can be finely tuned through G protein coupled receptors (GPCR), but the detailed mechanism how calcium channels are modulated through the activation of G proteins is still poorly understood. In this MSc thesis, the structural requirement for voltage-dependent modulation of Ca_v2 channels is explored using an invertebrate presynaptic calcium channel LCa_v2 . LCa_v2 does not share the same G protein modulation characteristics as $rCa_v2.2$, a mammalian homolog. Their differences serve as a basis for comparison in this study.

4.1 G protein modulation of presynaptic Ca_v2 calcium channels

Calcium ion entry through presynaptic Voltage Gated Calcium Channels (VGCC) is an essential step in neurotransmitter release. The Ca_v2 family of calcium channels include N-type ($Ca_v2.2$), P/Q-type ($Ca_v2.1$) and R-type ($Ca_v2.3$) channels. These different Ca_v2 genes are differentially distributed in presynaptic terminals, and vary in their inhibition by G proteins (Reid et al., 2003). G protein modulation through GPCRs such as GABA, adenosine A, dopamine and opioid receptors inhibit native calcium currents and reduce transmitter release, serving as an important means of adjusting presynaptic strength or preventing excessive transmission (Wu and Saggau, 1997). Although G protein modulation is present in both N-type and P/Q-type calcium channels, N-type channels display a stronger G protein inhibition than P/Q-type channels (Colecraft et al., 2000; Currie and Fox, 1997). Furthermore, different cell types express different quantities of N-type and P/Q-type calcium channels and

bear unique GPCR-coupled pathways for inhibiting calcium channels (Diverse-Pierluissi and Dunlap, 1993; Diverse-Pierluissi et al., 1995; Raingo et al., 2007; Shapiro and Hille, 1993). This greatly extends the capacity of G protein modulation in different cells.

Voltage dependent inhibition is the predominant form of G protein modulation. The G protein effect is sensitive to membrane potential, with less pronounced inhibition at a more depolarized potential. Voltage-sensitive modulation is mediated through the direct coupling of G $\beta\gamma$ subunits, providing a direct, rapid and reversible modulatory effect. The voltage dependent modulation can be relieved by strong depolarizations and bursts of action potential waveforms (Brody et al., 1997). This provides an activity-dependent relief of inhibition adjusted by neuronal firing frequency (Ikeda and Dunlap, 2007). Voltage-sensitive inhibition varies considerably between N-type and P/Q-type currents in presynaptic terminals and their differences in G protein modulation may contribute to differences in short time plasticity in different synapses (Colecraft et al., 2000; Currie and Fox, 1997; Currie and Fox, 2002).

A voltage independent G protein modulation has been identified in many preparations, which may utilize a distinct pathway (Diverse-Pierluissi et al., 1995; Raingo et al., 2007). Voltage independent modulation bears a slower onset and recovery rate, and provides a persistent inhibition independent of cellular activity. Voltage-dependent and independent components together diversify the possibilities for G protein modulation.

4.2 Expression of invertebrate LCa_v2 channel

Compared to multiple mammalian calcium channel isoforms, invertebrates including fruit fly (*Drosophila melanogaster*), Sea Hare (*Aplysia californica*) and nematode

(*Caenorhabditis elegans*) bear a single homolog representing multiple mammalian genes (Jeziorski et al., 2000). VGCC orthologs of *Lymnaea stagnalis* have been isolated, among which LCa_v2 is the representative of both mammalian N- and P/Q-type and responsible for neurotransmitter release (Spafford and Zamponi, 2003). In this research project, the LCa_v2 channel was subcloned into a bicistronic expression vector pIRES2-EGFP and expressed in human embryonic kidney HEK293T cells (Figure 6, Figure 8). HEK293T cell line was chosen because its endogenous VGCC expression level was low and it was amenable for patch clamp recording.

All recording were carried out at room temperature. It was suggested the recording temperature would affect channel activity. Increasing the temperature from 21°C to 37°C resulted in reduction in activation and inactivation time constant of T-type calcium channel (Iftinca et al., 2006). As snail belongs to poikilothermia animal, room temperature would better mimic the physiological environment of LCa_v2 calcium channel.

Analyses of the current-voltage relationships indicated that LCa_v2 (n=7) and its rat homolog $rCa_v2.2$ (n=6) shared nearly identical voltage sensitivities under the same conditions (20mM extracellular barium). Both channels began to activate around -20mV and reached the peak value around +20mV (Figure 11). $rCa_v2.2$ peaked at +10mV in similar condition (Roulet et al., 1999), and perhaps the deviation observed in our experiments might reflect the endogenous G protein expression in our system evident from the larger prepulse facilitation ratios (See discussion below). On the other hand, results from another lab (Yasuda et al., 2004) also showed a similar Current-Voltage peak at +20mV for $rCav2.2$ under the same condition. The current-voltage curve for LCa_v2 was almost identical to previous experiments studying

LCa_v2 with the N-terminus from *rCa_v2.1* (Spafford et al., 2003a). As action potential waves begin at approximately -50mV and peak at +40mV, the activities of *LCa_v2* and *rCa_v2.2* would both greatly be affected by neuron excitabilities. Similar voltage-sensitivities between invertebrate *LCa_v2* and mammalian *Ca_v2.2* channel may indicate conservation of the threshold and limits of voltage-dependent processes in neurons, such as synaptic transmission.

The time dependent inactivation decay and the voltage dependent inactivation decay of both channels were also compared (Figure 12, Figure 13). Barium was used as a charge replacing native calcium ion in the external solution to avoid activating calcium dependent processes, including potential calcium dependent inactivation of *Ca_v2* channels. In comparison, the kinetics of inactivation decay of *LCa_v2* at maximal current was significantly faster than that of *rCa_v2.2*. The fast component of inactivation decay was curve fit using a single exponential equation, with a tau value of 43.2 ± 1.22 ms for *LCa_v2* and was 130.6 ± 0.85 ms for *rCa_v2.2*. Typically, calcium channels have fast and slow components of inactivation decay, but only the fast component was determined here since the test pulse at peak current of +20mV was limited to 450ms, and not long enough to elaborate the other inactivating component. The faster inactivation decay might be a natural property of *LCa_v2*. One should consider that the calcium channels in HEK293T cells were evaluated at room temperature, (similar to the body temperature of snails) but much lower than the body temperature of mammals and the temperature of native rat channels (37°C). Perhaps, under native conditions, the inactivation decay of *rCa_v2.2* might resemble the inactivation decay of *LCa_v2* at room temperature. The kinetics of inactivation decay is also affected by the coexpression of *Ca_vβ* isoform, with highly variable results depending on which of four

mammalian beta subunits are expressed. A *Lymnaea* beta subunit of calcium channel $LCa_v\beta$ was shown to slow the kinetics of inactivation decay of LCa_v2 and $rCav2.2$ channels *in vitro* (Spafford et al., 2004) but multiple isoforms recently discovered in our lab may generate other possibilities for modulating inactivation properties (personal communication, Taylor Dawson).

The voltage dependence of channel availability was measured using steady state conditions for inactivation. The half inactivation potential, where half of the channels were inactivated after a 4 second depolarization, was calculated as $-39.8\text{mV}\pm 0.82$ for LCa_v2 and $-49.6\text{mV}\pm 1.45$ for $rCa_v2.2$ (Figure 13). Both data were in accordance to previous reports (Rouillet et al., 1999; Spafford et al., 2003a; Yasuda et al., 2004). However, with one replicate was conducted ($n=1$) each, more trials are suggested for statistic analysis.

To summarize, although LCa_v2 and $rCa_v2.2$ channels shared biophysical similarities, there are some differences. While equally responding to activation, LCa_v2 showed a depolarizing shift in voltage dependent inactivation and much faster inactivation decay.

4.3 LCa_v2 appears to lack voltage dependent G protein modulation

A major feature of voltage dependent G protein modulation is that the inhibition of calcium channel activity could be relieved by a strong depolarization. PPF ratio measured by dividing the peak current with a prepulse to the peak current without a prepulse in the paired pulse facilitation protocol could be used to depict the extent of voltage dependent G protein inhibition. If the ratio is significantly above one, the voltage dependent G protein inhibition is present. The PPF ratio below or at one for the invertebrate LCa_v2 channel implied a lack of

apparent voltage-dependent G protein modulation (Figure 15). $rCa_v2.2$ had PPF ratios significantly above unity. The highest values was $rCa_v2.2$ with the coexpression of exogenous $G\beta_1\gamma_2$ subunits (1.95 ± 0.11 , $n=8$) compared to PPF ratio relying on lower endogenous G protein expression in HEK293T cells (1.37 ± 0.07 , $n=9$). The presence of exogenous $G\beta_1\gamma_2$ subunits was significant over endogenous background for evaluation of G protein modulation of $rCa_v2.2$ in a Turkey Test (at a 95% percent confidence level). PPF ratios were 1.00 ± 0.03 ($n=8$) and 0.95 ± 0.03 ($n=7$) for LCa_v2 and were not significantly different with or without exogenous expression of G proteins respectively.

An interesting finding was that PPF ratios determined for LCa_v2 were sometimes below unity (Table 2). The lower than unity ratios have previously been attributed to a greater channel inactivation after a strong depolarizing prepulse, which is apparently masked during the G protein inhibition (Currie and Fox, 2002).

Another key feature of channels undergoing voltage-dependent G protein modulation is a slowing of activation rate as the binding of $G\beta\gamma$ subunits retards the channel openings. Calcium channels would change from a “willing to open” mode to a “reluctant to open” mode when inhibited by G proteins, so that channel are not easily opened by small or moderate depolarizations (Bean, 1989). This is evident when comparing sample traces of facilitation (eg. Figure 14). Without a depolarizing prepulse, and thus under G protein inhibition, $rCa_v2.2$ currents evaluated with coexpressed $G\beta_1\gamma_2$ subunits activated much more slowly compared to the current elicited after a strong depolarizing prepulse which temporarily relieved the G protein inhibition. Notice that LCa_v2 traces do not have altered slow activation kinetics under the same conditions. This is a one of the indicators besides PPF ratios that suggest an absence

of voltage dependent G protein modulation of LCa_v2 channels. In the future work, the role of $G\beta\gamma$ subunits could be confirmed by coexpressing β -ARK peptide which contains the $G\beta\gamma$ binding region of the β -Adrenergic Receptor Kinase (Tomblin et al., 2006), and G protein modulation of LCa_v2 could also be explored by activating G protein coupled receptors such as mu-opioid receptor.

One possibility for the absence of voltage-dependent G protein modulation is that invertebrate LCa_v2 might not be coupling to G protein subunits *in vitro* because they are mammalian instead of native snail ones. To explore this, an invertebrate $G\beta$ subunit $LG\beta_1$ was isolated from *Lymnaea stagnalis* (cloned by MSc student, Taylor Dawson in the lab) and was coexpressed with calcium channel subunits and rat G protein gamma2 subunit. PPF ratios were determined electrophysiologically (Figure 16). The preliminary PPF ratio data gathered (1.02 ± 0.117 ($n=2$)) indicated that LCa_v2 still lacked the voltage dependent G protein modulation property even with coexpressed *Lymnaea* G protein subunit, $LG\beta_1$. Perhaps this is not surprising, given that nifedipine-insensitive calcium currents in identified *Lymnaea* neurons (such as VD4) also lacked endogenous voltage-dependent G protein modulation (McCamphill et al. 2007 and Spafford, unpublished).

A positive control using *in vitro* biochemistry and/or electrophysiological experiments will have to be performed to confirm that the *in vitro* expressed $LG\beta_1$ subunits form expressed proteins that will functionally interact with other proteins. For example, western blot might be performed to detect the expression of , and co-immunoprecipitation could be used to study the interaction between calcium channels and G beta subunit, while G protein-activated inwardly rectifying (GIRK) potassium channels, whose conductance would be enhanced by functional

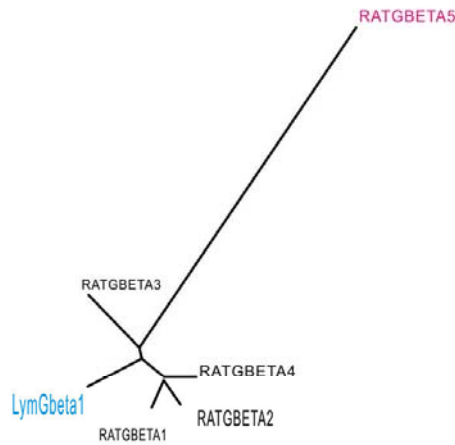
G $\beta\gamma$ subunits, could serve as a surrogate that others have used to indicate functionality of *in vitro* expressed G proteins (Doering et al., 2004).

Interestingly, when LG β_1 was coexpressed with rCa $_v$ 2.2, the PPF ratio was 1.33 \pm 0.1 (n=3), and not significantly different from the endogenous mammalian G protein modulation in HEK293T cells. This suggests that LG β_1 did not functionally modulate rCa $_v$ 2.2 over the endogenous G protein background in HEK293T cells. If LG β_1 was well expressed in our system, it would be an unexpected finding that the invertebrate G protein beta subunit LG β_1 also does not appear to be compatible with voltage-dependent G protein modulation in addition to the invertebrate Ca $_v$ 2 calcium channel. Previously, Arnot and colleagues demonstrated that different G β subunit genes have differing capacities for G protein facilitation of Ca $_v$ 2.2 channels. It was reported that G β_5 was phylogenetically more distant from the other four G protein beta subunits (G β 1 to 4) and was unable to modulate N-type calcium channel (Arnot et al., 2000). A phylogenetic tree derived from amino acids sequence alignment (Figure 26 A) indicates that LG β_1 is closer to the calcium channel modulating G proteins (G β 1-G β 4) and more distant from the mammalian G protein subunit that does not interact with calcium channels, G β 5. Although G γ subunit might affect the function of G β , it was assumed it was G β that played a major role in G protein inhibition and exogenous expression work also indicated G γ 2 subunit could associate with most G β subunits (Arnot et al., 2000; Ruiz-Velasco and Ikeda, 2000; Zhou et al., 2000), indicating invertebrate LG β should be able to associate mammalian rG γ 2. Mutagenesis work by Doering and colleagues involved swapping regions between G β 1 and G β 5 to identify the critical residues in mammalian G β 1 responsible for voltage dependent G protein modulation (Doering et al.,

2004). Asn-110, Tyr-111, Val-112, residues 140-168 and 186-204 were considered important, and later, Tedford and colleagues suggested that Ser-189 was a particularly critical residue (Tedford et al., 2006). Comparisons between *Lymnaea* G β_1 and equivalent mammalian G proteins using a sequence alignment (Figure 26 B) indicates that replacements of Gln156, Leu192 and Thr196 in rat G beta 1 subunit, which is greatly different from residues in the similar positions in LG β , might cause the loss of binding/modulation property of LG β_1 . These are three residues within the regions outlined by Doering and colleagues that were important for G protein modulation with rat G beta 1. Structural determinants for the possible absence of modulation of LG β_1 can be determined by future mutagenesis studies involving swapping residues in homologous positions like Thr196 into LG β_1 and assessing the possible gain of G protein modulation as a result of the mutagenesis.

Figure 26: Sequence alignment of invertebrate (*Lymnaea*) G β 1 subunit and rat G β subunit homologs (rat G β 1-4). Panel A shows the phylogenetic tree based on amino acid sequences. Branch lengths represent probable evolutionary distance. Panel B illustrates the sequence alignment of G protein candidates for voltage dependent G protein modulation. The location of the last amino acid of each line is numbered. Dark and lighter grey-shaded amino acids represent identical and positive matches, respectively in the sequence alignment. Black boxes indicate the region of residues 110-112, residues 140-168 and residues 186-204 that have been described in previous studies to be critical for voltage-dependent G protein modulation of calcium channels. Amino acid residues within these outlined black boxes with little conservation in *LG β 1* but are conserved in homologous mammalian G proteins are indicated in red. These three residues are Gln156, Leu192 and Thr196 in *rG β 1* respectively. For future experiments, these three amino acids are excellent candidates for examination by site directed mutagenesis for their potential roles in voltage-dependent G protein modulation.

A



B

z0p1	MSNDLEALKROET EOLKNOIR EAKFAAGDT TLAQACSOVEAVGR IQMRTKRTLROHLAKIY	60
r0p1	MS-ELDQLRQEA EOLKNOIR DAKFACADATLSQITNNIDPVGR IQMRTKRTLROHLAKIY	59
r0p2	MS-ELDQLRQEA EOLRNOIR DAKFACADGSLTQITAGLDPVGR IQMRTKRTLROHLAKIY	59
r0p3	MG-EMEQLRQEA EOLKNOIR DAKFACADITLAEVLSGLELVGR IQMRTKRTLROHLAKIY	59
r0p4	MS-ELDQLRQEA EOLRNOIR DAKFACADATLVQITSNMDSVGR IQMRTKRTLROHLAKIY	59
z0p1	AMHDAS QSRN LVSASODGELLVDDG YTTNEVHA IPLESSDVMTCAAYAPSGNFMACCGOLDN	120
r0p1	AMHDGTSRLLVVSASODGELLVDDG YTTNEVHA IPLESSDVMTCAAYAPSGNFMACCGOLDN	119
r0p2	AMHDGTSRLLVVSASODGELLVDDG YTTNEVHA IPLESSDVMTCAAYAPSGNFMACCGOLDN	119
r0p3	AMHDATSRLLVVSASODGELLVDDG YTTNEVHA IPLESSDVMTCAAYAPSGNFMACCGOLDN	119
r0p4	AMHDGYSRLLVVSASODGELLVDDG YTTNEVHA IPLESSDVMTCAAYAPSGNFMACCGOLDN	119
z0p1	ICCIYS LETREGNVKVERELPGHTOYLSOCFFLDDNSIVTSSGDMSCALDDIETGQQTTT	190
r0p1	ICCIYN LETREGNVKVERELAGHTOYLSOCFFLDDNQIVTSSGDTTCALDDIETGQQTTT	179
r0p2	ICCIYS LETREGNVKVERELPGHTOYLSOCFFLDDNQIVTSSGDTTCALDDIETGQQTVG	179
r0p3	MCCIYS LISREGNVKVERELSAHTOYLSOCFFLDDNNIVTSSGDTTCALDDIETGQQITV	179
r0p4	ICCIYN LETREGNVKVERELPGHTOYLSOCFFLDDNQIVTSSGDTTCALDDIETGQQTTT	179
z0p1	FTQHTGQVHSLSTSPDFRTFVSGACDASAEFLUDVREGMCKOTFSQHESDINAITYFPNQH	240
r0p1	FTQHTGQVHSLSLAPDTRFLVSGACDASAEFLUDVREGMCKROTFTQHESDINAICFFPNQN	239
r0p2	FAGHSQQVHSLSLAPDTRFLVSGACDASAEFLUDVREGMCKROTFTQHESDINAVAFFPNQY	239
r0p3	FVGHGQVHSLAVSPDYKLFVSGACDASAEFLUDVREGTCROTFTQHESDINAICFFPNQE	239
r0p4	FTQHTGQVHSLSLAPDTRFLVSGACDASAEFLUDVREGMCKROTFTQHESDINAVAFFPNQY	239
z0p1	AFAFGSDDATCRLFDLEADDELMTYSHDNICGITYVAFSEKGRLLLAGYDDFHCNVDDV	300
r0p1	AFAFGSDDATCRLFDLEADDELMTYSHDNICGITYVAFSEKGRLLLAGYDDFHCNVDDA	299
r0p2	AFTFGSDDATCRLFDLEADDELMTYSHDNICGITYVAFSEKGRLLLAGYDDFHCNVDDA	299
r0p3	AICFGSDDATCRLFDLEADDELTA YSHDNICGITYVAFSEKGRLLLAGYDDFHCNVDDA	299
r0p4	AFAFGSDDATCRLFDLEADDELLYSHDNICGITYVAFSEKGRLLLAGYDDFHCNVDDA	299
z0p1	LKQETHCVLA GHDNFVSCLOVTE DGS AVATGSD DDFL IUN	341
r0p1	LNADRAQVLA GHDNFVSCLOVTE DDM AVATGSD DDFL IUN	340
r0p2	MKGDRAQVLA GHDNFVSCLOVTE DDM AVATGSD DDFL IUN	340
r0p3	LKCEVQVLS GHDNFVSCLOVTE DDM AVATGSD DDFL IUN	340
r0p4	LKGGRSQVLA GHDNFVSCLOVTE DDM AVATGSD DDFL IUN	340

4.4 N-terminus and I-II linker of *rCa_v2.2* alone did not confer voltage dependent G protein modulation to *LCa_v2* calcium channels

In previous reports, the N-terminus and I-II linker in mammalian Ca_v2 channel homologs were found to play a role in voltage-dependent G protein modulation (Agler et al., 2005; Bourinet et al., 1996; Zamponi et al., 1997). To identify the determinants for voltage-dependent G protein modulation, chimeras were constructed by swapping N-terminus and I-II linker from *rCa_v2.2* into *LCa_v2*. Unique restriction sites were created using QuikChange Mutagenesis PCR, which served as a rapid method to introduce new restriction sites delimiting the regions to be swapped without changing the amino acid coding sequence. Both chimeras were successfully created and expressed. Interestingly, the chimeras with rat sequences, especially the N-terminal chimera *LCa_v2* (_{R1L2L3L4}) expressed better than the wild type *LCa_v2* calcium channel. This was probably because the mammalian N-terminal sequence may have been more compatible with our mammalian expression system. Possibilities include that the N-terminal sequence may have increased the efficiency of transcription or translation or possibly the membrane targeting of *LCa_v2* channels (Spafford et al., 2003a).

The calculated PPF ratios indicated these two mammalian regions (i.e. the N-terminus and I-II linker) separately did not create a voltage dependent G protein modulation in the *LCa_v2* calcium channel (Figure 25). Both the N-terminus or the I-II linker have been implicated as the G protein binding site by knock down or disruption of either of these two regions separately (De Waard et al., 1997; Zamponi et al., 1997). Our findings may be more consistent with the more recent work by Agler et al. proposing a cooperative interaction between N-terminus and I-II linker participating in Gβγ mediated voltage dependent

modulation (Agler et al., 2005). In future work, a double mutant with both N-terminus and I-II linker region from *rCa_v2.2* in *LCav2* will be constructed to address whether both domains participate cooperatively in voltage dependent G protein modulation.

4.5 *LCa_v2* as a model to study VD/VI G protein modulation

Although the invertebrate *LCa_v2* calcium channel lacks voltage dependent G protein modulation, recent work suggests that snail *LCa_v2* currents can be depressed by G proteins. For example, when a constitutive-activator of G proteins GTP- γ S, was included in the internal solution contained in the patch pipette, no *LCa_v2* currents could be detected. Then when the same drug (GTP- γ S) was dialyzed, *LCa_v2* mediated barium currents were observed at first and then irreversibly ran down quickly and could not be relieved by repeated strong depolarizations (Spafford et al., 2003a). A similar G protein inhibition is apparent in cultured *Lymnaea* VD4 neurons. Patrick McCamphill (a PhD student in our lab) recently reported that application of serotonin to *Lymnaea* VD4 neurons inhibited presynaptic calcium currents by a mechanism that is sensitive to GDP-beta-S, an inhibitor of G protein activation. It is unlikely that this regulation is voltage-dependent, as the serotonin mediated inhibition in snails was likely mediated by the cytoplasmic second messenger pathway involving cAMP, and not a direct calcium channel inhibition from liberated G beta gamma subunits (McCamphill et al., 2008).

Interestingly, a possibly comparable voltage-insensitive G protein mechanism has been identified in mammals in pain sensory neurons of the dorsal root ganglia and sympathetic ganglia (Bernheim et al., 1991; Diverse-Pierluissi et al., 1995; Raingo et al., 2007). These

mechanisms in mammals appear to involve different G protein-mediated pathways, and different regions of calcium channels than the ubiquitous membrane-delimited, $G\beta\gamma$ mediated, voltage-dependent form of G protein modulation. It was proposed recently the tyrosine 1743 and tyrosine 1747 in the C terminus of $rCa_v2.2$ were essential for voltage independent G protein modulation through a tyrosine kinase pathway (Raingo et al., 2007). Interestingly, both tyrosine residues are found in a similar position in the C terminus of LCa_v2 . It is supposed the lack of necessary N-terminus/I-II linker interaction retarded the voltage dependent inhibition by $G\beta\gamma$ while we hypothesis that the conserved tyrosine residues in the C-terminus confers the ability of LCa_v2 to be modulated by $G\alpha$ in a voltage-independent way. As LCa_v2 channel has an inherent voltage-independent G protein modulation, it will be interesting to address what is the consequence of heterologous expression of the chimeric presynaptic LCa_v2 channel with a voltage-dependent G protein modulatory site on the transmitter release modulation in invertebrate synapses. Mammalian neurons contain a ubiquitous, voltage-dependent, G protein modulation, so only an invertebrate model provides an opportunity to address a potential gain-of-function of voltage-dependent G protein regulation.

4.6 Summary

In this project, an invertebrate voltage gated calcium channel (LCa_v2) isolated from the pond snail *Lymnaea stagnalis* was expressed *in vitro* and characterized. While it showed similar biophysical properties as its mammalian homolog $rCa_v2.2$ channel, LCa_v2 lacks the mammalian-type voltage dependent G protein modulation. Analyses of chimeric channels

indicated the N-terminus or I-II linker region from *rCa_v2.2* alone was not enough to confer the voltage-dependent G protein modulation in *LCa_v2*. Furthermore, the *Lymnaea* G protein beta subunit did not appear to be compatible with mammalian-type, voltage-dependent G protein modulation.

Overall Significance:

My research suggests that the voltage-dependent form of G protein modulation is not found in a representative invertebrate and thus may have arisen as a specialization in vertebrates. The potential more ancient voltage independent mechanism, is slower in onset and recovery, and is inhibitory without influence from cellular activity. Since the voltage-independent regulation appears to be amplified through the secondary messenger pathway, it is thus a highly-sensitive mechanism of inhibition requiring relatively low neurotransmitter concentration and receptor occupancy of the G protein coupled receptor to have a potent effect.

In comparison, the voltage dependent G protein modulation is a dynamic and rapid form of calcium channel modulation that may alter synaptic strength. The rate and extent of inhibition of this form is proportional to the stimulus frequency. It also serves as a high pass filter, allowing only the strongest trains of action potentials to relieve inhibition and activate synaptic calcium channels. Vertebrates likely gained this voltage dependent G protein modulation during evolution to provide greater capacity for integration of nerve network signaling pathways. Having both voltage-dependent and voltage-independent modulation in the same cell diversifies the possibilities for modulation of synaptic activity. For example, the

voltage independent modulation is more enriched in nociceptive neurons to promote the possibilities for strong analgesic responses through opiate activation of G protein coupled receptors. In comparison, voltage dependent modulation might be involved in short-term activity dependent changes such as the laying down of short-term memory. Voltage dependent modulation responds faster and self-adjusts more frequently and greatly extends the fine tuning ability in response to fluctuations in neural excitability.

Future work:

In future work, more chimeric channels will be made from *rCav2.2* channels to create a voltage-dependent G protein modulation site in *LCav2* channels to address its minimal structural requirements. The first step will be to assess whether the double mutant with both N-terminus and I-II linker regions from *rCa_v2.2* will be enough to support voltage dependent G protein modulation. Future work may also include a closer examination of the endogenous voltage-independent G protein modulation of *LCav2* channels by overexpression G protein coupled receptors (GPCRs) such as u-opioid receptor or dopamine receptor. This *in vitro* work will be paired with neuronal work in identified presynaptic neurons and synapses to address the neuronal consequences of voltage-independent G protein modulation.

Appendix 1: List of primers

Primer 1#, LCav2 SpeI f	5-GGA TCC CGG GTC AAC ACC AGT CAT CGT CAT CTT C-3
Primer 2#, LCav2CT-XmaI	5-GCT CAC AGA ACT AGT GGC TAT CCA C-3
Primer 3#, Mega with SfuI	5-GAA TGG GGG CCA TTC GAA TAC ATG GTG CTA CTC AC-3
Primer 4#, Mega with SfuI AS	5-GTG AGT AGC ACC ATG TAT TCG AAT GGC CCC CAT TC-3
Primer 5#, Mega with BamHI	5-CAC TCA TCA TAC TGG GAT CCT TCT TCA TGC TAA ATC TAG-3
Primer 6#, Mega with BamHI AS	5-CTA GAT TTA GCA TGA AGA AGG ATC CCA GTA TGA TGA GTG-3
Primer 7#, Mega with SpeI	5-GGT ACT CTA TAA GAC GAC TAG TGA AAA GCC AGC TTT-3
Primer 8#, Mega with SpeI AS	5-AGA AAA GCT GGC TTT TCA CTA GTC GTC TTA TAG AGT-3
Primer 9#, Ra1b BamHI f	5-CAT TGG ATC CTT CTT CAT GCT CAA CCTG-3
Primer 10#, Ra1b SpeI b	5-TTT CAC TAG TCG ACG GAT AAG GAA CCG-3

Appendix 2: List of original recording data

Figure 9: This figure was generated from the recording: 07619005.

Figure 10: This figure was generated from the recording 07611004.

Figure 11: This figure was generated from the recordings of 07611004, 07619006, 07619013, 07625013, 08211007, 08402015, 08507018 and 07617001, 07618006, 07621030, 08402003, 08623006, 08623012.

Figure 12: This figure was generated from the recordings of 07611003, 07619005, 07619012, 07625010, 08205007, 08211005, 08402011, 08507016 and 07617000, 07621029, 08116002, 08208001, 08402000, 08518007, 08623004, 08623010.

Figure 13: This figure was generated from recordings 08508000 and 08623014.

Figure 14: This figure was generated from recordings 07626007 and 07621041.

Figure 15: This figure was generated based on recordings of: 07611005, 07619007, 07619014, 07625011, 08205010, 08211006, 08402013, 08507017; 07626007, 07730005, 07730010, 07811005, 07828001, 07831001, 07831013; 07617002, 07618004, 07621032, 08116001, 08208003, 08402001, 08518005, 08623005, 08623011 and 07620002, 07621041, 07711004, 07723001, 07812001, 08502003, 08602014, 08602022.

Figure 16: This figure was generated from recordings 08304013, 08409028 and 08418003, 08420004, 08415002.

Figure 25: This figure was generated from recordings 08228011, 082280016; 08225003, 08225010, 08409004, 08409012, 08303015 and 08706005, 08707028.

References:

- Agler, H. L., Evans, J., Tay, L. H., Anderson, M. J., Colecraft, H. M., and Yue, D. T. (2005). G protein-gated inhibitory module of N-type (ca(v)2.2) ca²⁺ channels. *Neuron* *46*, 891-904.
- Arikkath, J., and Campbell, K. P. (2003). Auxiliary subunits: essential components of the voltage-gated calcium channel complex. *Curr Opin Neurobiol* *13*, 298-307.
- Arnot, M. I., Stotz, S. C., Jarvis, S. E., and Zamponi, G. W. (2000). Differential modulation of N-type 1B and P/Q-type 1A calcium channels by different G protein subunit isoforms. *J Physiol* *527 Pt 2*, 203-212.
- Bean, B. P. (1989). Neurotransmitter inhibition of neuronal calcium currents by changes in channel voltage dependence. *Nature* *340*, 153-156.
- Bell, T. J., Thaler, C., Castiglioni, A. J., Helton, T. D., and Lipscombe, D. (2004). Cell-specific alternative splicing increases calcium channel current density in the pain pathway. *Neuron* *41*, 127-138.
- Berjukow, S., Doring, F., Froschmayr, M., Grabner, M., Glossmann, H., and Hering, S. (1996). Endogenous calcium channels in human embryonic kidney (HEK293) cells. *Br J Pharmacol* *118*, 748-754.
- Bernheim, L., Beech, D. J., and Hille, B. (1991). A diffusible second messenger mediates one of the pathways coupling receptors to calcium channels in rat sympathetic neurons. *Neuron* *6*, 859-867.
- Bichet, D., Cornet, V., Geib, S., Carlier, E., Volsen, S., Hoshi, T., Mori, Y., and De Waard, M. (2000). The I-II loop of the Ca²⁺ channel alpha1 subunit contains an endoplasmic reticulum retention signal antagonized by the beta subunit. *Neuron* *25*, 177-190.

- Bourinet, E., Soong, T. W., Stea, A., and Snutch, T. P. (1996). Determinants of the G protein-dependent opioid modulation of neuronal calcium channels. *Proc Natl Acad Sci U S A* 93, 1486-1491.
- Bouvier, M. (2001). Oligomerization of G-protein-coupled transmitter receptors. *Nat Rev Neurosci* 2, 274-286.
- Brody, D. L., Patil, P. G., Mulle, J. G., Snutch, T. P., and Yue, D. T. (1997). Bursts of action potential waveforms relieve G-protein inhibition of recombinant P/Q-type Ca²⁺ channels in HEK 293 cells. *J Physiol* 499 (Pt 3), 637-644.
- Campbell, V., Berrow, N. S., Fitzgerald, E. M., Brickley, K., and Dolphin, A. C. (1995). Inhibition of the interaction of G protein G(o) with calcium channels by the calcium channel beta-subunit in rat neurones. *J Physiol* 485 (Pt 2), 365-372.
- Catterall, W. A. (2000). Structure and regulation of voltage-gated Ca²⁺ channels. *Annu Rev Cell Dev Biol* 16, 521-555.
- Chase, R. (2002). *Behavior and Its Neural Control in Gastropod Molluscs* (New York, Oxford University Press).
- Clapham, D. E., and Neer, E. J. (1997). G protein beta gamma subunits. *Annu Rev Pharmacol Toxicol* 37, 167-203.
- Colecraft, H. M., Patil, P. G., and Yue, D. T. (2000). Differential occurrence of reluctant openings in G-protein-inhibited N- and P/Q-type calcium channels. *J Gen Physiol* 115, 175-192.
- Cox, D. H., and Dunlap, K. (1992). Pharmacological discrimination of N-type from L-type calcium current and its selective modulation by transmitters. *J Neurosci* 12, 906-914.

- Currie, K. P., and Fox, A. P. (1997). Comparison of N- and P/Q-type voltage-gated calcium channel current inhibition. *J Neurosci* *17*, 4570-4579.
- Currie, K. P., and Fox, A. P. (2002). Differential facilitation of N- and P/Q-type calcium channels during trains of action potential-like waveforms. *J Physiol* *539*, 419-431.
- De Waard, M., Liu, H., Walker, D., Scott, V. E., Gurnett, C. A., and Campbell, K. P. (1997). Direct binding of G-protein betagamma complex to voltage-dependent calcium channels. *Nature* *385*, 446-450.
- Diverse-Pierluissi, M., and Dunlap, K. (1993). Distinct, convergent second messenger pathways modulate neuronal calcium currents. *Neuron* *10*, 753-760.
- Diverse-Pierluissi, M., Goldsmith, P. K., and Dunlap, K. (1995). Transmitter-mediated inhibition of N-type calcium channels in sensory neurons involves multiple GTP-binding proteins and subunits. *Neuron* *14*, 191-200.
- Doering, C. J., Kisilevsky, A. E., Feng, Z. P., Arnot, M. I., Peloquin, J., Hamid, J., Barr, W., Nirdosh, A., Simms, B., Winkfein, R. J., and Zamponi, G. W. (2004). A single Gbeta subunit locus controls cross-talk between protein kinase C and G protein regulation of N-type calcium channels. *J Biol Chem* *279*, 29709-29717.
- Dolphin, A. C. (1995). The G.L. Brown Prize Lecture. Voltage-dependent calcium channels and their modulation by neurotransmitters and G proteins. *Exp Physiol* *80*, 1-36.
- Dolphin, A. C. (2003). G protein modulation of voltage-gated calcium channels. *Pharmacol Rev* *55*, 607-627.
- Dolphin, A. C. (2006). A short history of voltage-gated calcium channels. *Br J Pharmacol* *147 Suppl 1*, S56-62.

Dolphin, A. C., Page, K. M., Berrow, N. S., Stephens, G. J., and Canti, C. (1999). Dissection of the calcium channel domains responsible for modulation of neuronal voltage-dependent calcium channels by G proteins. *Ann N Y Acad Sci* 868, 160-174.

Dunlap, K., and Fischbach, G. D. (1981). Neurotransmitters decrease the calcium conductance activated by depolarization of embryonic chick sensory neurones. *J Physiol* 317, 519-535.

Ertel, E. A., Campbell, K. P., Harpold, M. M., Hofmann, F., Mori, Y., Perez-Reyes, E., Schwartz, A., Snutch, T. P., Tanabe, T., Birnbaumer, L., *et al.* (2000). Nomenclature of voltage-gated calcium channels. *Neuron* 25, 533-535.

Fields, H. L., Heinricher, M. M., and Mason, P. (1991). Neurotransmitters in nociceptive modulatory circuits. *Annu Rev Neurosci* 14, 219-245.

Gurnett, C. A., Felix, R., and Campbell, K. P. (1997). Extracellular interaction of the voltage-dependent Ca²⁺ channel alpha2delta and alpha1 subunits. *J Biol Chem* 272, 18508-18512.

Hepler, J. R., and Gilman, A. G. (1992). G proteins. *Trends Biochem Sci* 17, 383-387.

Herlitze, S., Garcia, D. E., Mackie, K., Hille, B., Scheuer, T., and Catterall, W. A. (1996). Modulation of Ca²⁺ channels by G-protein beta gamma subunits. *Nature* 380, 258-262.

Hille, B. (1994). Modulation of ion-channel function by G-protein-coupled receptors. *Trends Neurosci* 17, 531-536.

Hodgkin, A. L., and Huxley, A. F. (1952). A quantitative description of membrane current and its application to conduction and excitation in nerve. *J Physiol* 117, 500-544.

Holz, G. G. t., Rane, S. G., and Dunlap, K. (1986). GTP-binding proteins mediate transmitter inhibition of voltage-dependent calcium channels. *Nature* 319, 670-672.

- Hyman, S. E. (2005). Neurotransmitters. *Curr Biol* *15*, R154-158.
- Iftinca, M., McKay, B. E., Snutch, T. P., McRory, J. E., Turner, R. W., and Zamponi, G. W. (2006). Temperature dependence of T-type calcium channel gating. *Neuroscience* *142*, 1031-1042.
- Ikeda, S. R. (1991). Double-pulse calcium channel current facilitation in adult rat sympathetic neurones. *J Physiol* *439*, 181-214.
- Ikeda, S. R. (1996). Voltage-dependent modulation of N-type calcium channels by G-protein beta gamma subunits. *Nature* *380*, 255-258.
- Ikeda, S. R., and Dunlap, K. (2007). Calcium channels diversify their signaling portfolio. *Nat Neurosci* *10*, 269-271.
- Jeziorski, M. C., Greenberg, R. M., and Anderson, P. A. (2000). The molecular biology of invertebrate voltage-gated Ca(2+) channels. *J Exp Biol* *203*, 841-856.
- Kandel, E. R. (2004). The molecular biology of memory storage: a dialog between genes and synapses. *Biosci Rep* *24*, 475-522.
- Letts, V. A., Felix, R., Biddlecome, G. H., Arikath, J., Mahaffey, C. L., Valenzuela, A., Bartlett, F. S., 2nd, Mori, Y., Campbell, K. P., and Frankel, W. N. (1998). The mouse stargazer gene encodes a neuronal Ca²⁺-channel gamma subunit. *Nat Genet* *19*, 340-347.
- McCamphill, P. K., Dunn, T. W., and Syed, N. I. (2008). Serotonin modulates transmitter release at central Lymnaea synapses through a G-protein-coupled and cAMP-mediated pathway. *Eur J Neurosci* *27*, 2033-2042.
- McCleskey, E. W. (1994). Calcium channels: cellular roles and molecular mechanisms. *Curr Opin Neurobiol* *4*, 304-312.

Mochida, S., Sheng, Z. H., Baker, C., Kobayashi, H., and Catterall, W. A. (1996). Inhibition of neurotransmission by peptides containing the synaptic protein interaction site of N-type Ca²⁺ channels. *Neuron* *17*, 781-788.

Moroz, L. L., Edwards, J. R., Puthanveetil, S. V., Kohn, A. B., Ha, T., Heyland, A., Knudsen, B., Sahni, A., Yu, F., Liu, L., *et al.* (2006). Neuronal transcriptome of aplysia: neuronal compartments and circuitry. *Cell* *127*, 1453-1467.

Myhrer, T. (2003). Neurotransmitter systems involved in learning and memory in the rat: a meta-analysis based on studies of four behavioral tasks. *Brain Res Brain Res Rev* *41*, 268-287.

Newcomb, R., Szoke, B., Palma, A., Wang, G., Chen, X., Hopkins, W., Cong, R., Miller, J., Urge, L., Tarczy-Hornoch, K., *et al.* (1998). Selective peptide antagonist of the class E calcium channel from the venom of the tarantula *Hysterocrates gigas*. *Biochemistry* *37*, 15353-15362.

Page, K. M., Canti, C., Stephens, G. J., Berrow, N. S., and Dolphin, A. C. (1998). Identification of the amino terminus of neuronal Ca²⁺ channel alpha1 subunits alpha1B and alpha1E as an essential determinant of G-protein modulation. *J Neurosci* *18*, 4815-4824.

Qin, N., Platano, D., Olcese, R., Stefani, E., and Birnbaumer, L. (1997). Direct interaction of gbetagamma with a C-terminal gbetagamma-binding domain of the Ca²⁺ channel alpha1 subunit is responsible for channel inhibition by G protein-coupled receptors. *Proc Natl Acad Sci U S A* *94*, 8866-8871.

Raingo, J., Castiglioni, A. J., and Lipscombe, D. (2007). Alternative splicing controls G protein-dependent inhibition of N-type calcium channels in nociceptors. *Nat Neurosci* *10*,

285-292.

Reid, C. A., Bekkers, J. M., and Clements, J. D. (2003). Presynaptic Ca²⁺ channels: a functional patchwork. *Trends Neurosci* 26, 683-687.

Roulet, J. B., Spaetgens, R. L., Burlingame, T., Feng, Z. P., and Zamponi, G. W. (1999). Modulation of neuronal voltage-gated calcium channels by farnesol. *J Biol Chem* 274, 25439-25446.

Ruiz-Velasco, V., and Ikeda, S. R. (2000). Multiple G-protein betagamma combinations produce voltage-dependent inhibition of N-type calcium channels in rat superior cervical ganglion neurons. *J Neurosci* 20, 2183-2191.

Schiff, M. L., Siderovski, D. P., Jordan, J. D., Brothers, G., Snow, B., De Vries, L., Ortiz, D. F., and Diverse-Pierluissi, M. (2000). Tyrosine-kinase-dependent recruitment of RGS12 to the N-type calcium channel. *Nature* 408, 723-727.

Shapiro, M. S., and Hille, B. (1993). Substance P and somatostatin inhibit calcium channels in rat sympathetic neurons via different G protein pathways. *Neuron* 10, 11-20.

Sheng, Z. H., Westenbroek, R. E., and Catterall, W. A. (1998). Physical link and functional coupling of presynaptic calcium channels and the synaptic vesicle docking/fusion machinery. *J Bioenerg Biomembr* 30, 335-345.

Spafford, J. D., Chen, L., Feng, Z. P., Smit, A. B., and Zamponi, G. W. (2003a). Expression and modulation of an invertebrate presynaptic calcium channel alpha1 subunit homolog. *J Biol Chem* 278, 21178-21187.

Spafford, J. D., Dunn, T., Smit, A. B., Syed, N. I., and Zamponi, G. W. (2006). In vitro characterization of L-type calcium channels and their contribution to firing behavior in

invertebrate respiratory neurons. *J Neurophysiol* 95, 42-52.

Spafford, J. D., Munno, D. W., Van Nierop, P., Feng, Z. P., Jarvis, S. E., Gallin, W. J., Smit, A. B., Zamponi, G. W., and Syed, N. I. (2003b). Calcium channel structural determinants of synaptic transmission between identified invertebrate neurons. *J Biol Chem* 278, 4258-4267.

Spafford, J. D., Van Minnen, J., Larsen, P., Smit, A. B., Syed, N. I., and Zamponi, G. W. (2004). Uncoupling of calcium channel alpha 1 and beta subunits in developing neurons. *J Biol Chem* 279, 41157-41167.

Spafford, J. D., and Zamponi, G. W. (2003). Functional interactions between presynaptic calcium channels and the neurotransmitter release machinery. *Curr Opin Neurobiol* 13, 308-314.

Takahashi, T., and Momiyama, A. (1993). Different types of calcium channels mediate central synaptic transmission. *Nature* 366, 156-158.

Tanaka, H., and Shigenobu, K. (2005). Pathophysiological significance of T-type Ca²⁺ channels: T-type Ca²⁺ channels and drug development. *J Pharmacol Sci* 99, 214-220.

Tedford, H. W., Kisilevsky, A. E., Peloquin, J. B., and Zamponi, G. W. (2006). Scanning mutagenesis reveals a role for serine 189 of the heterotrimeric G-protein beta 1 subunit in the inhibition of N-type calcium channels. *J Neurophysiol* 96, 465-470.

Tedford, H. W., and Zamponi, G. W. (2006). Direct G protein modulation of Cav2 calcium channels. *Pharmacol Rev* 58, 837-862.

Thomas, P., and Smart, T. G. (2005). HEK293 cell line: a vehicle for the expression of recombinant proteins. *J Pharmacol Toxicol Methods* 51, 187-200.

Tombler, E., Cabanilla, N. J., Carman, P., Permaul, N., Hall, J. J., Richman, R. W., Lee, J.,

Rodriguez, J., Felsenfeld, D. P., Hennigan, R. F., and Diverse-Pierluissi, M. A. (2006). G protein-induced trafficking of voltage-dependent calcium channels. *J Biol Chem* *281*, 1827-1839.

Tsien, R. W., Ellinor, P. T., and Horne, W. A. (1991). Molecular diversity of voltage-dependent Ca²⁺ channels. *Trends Pharmacol Sci* *12*, 349-354.

Westenbroek, R. E., Hell, J. W., Warner, C., Dubel, S. J., Snutch, T. P., and Catterall, W. A. (1992). Biochemical properties and subcellular distribution of an N-type calcium channel alpha 1 subunit. *Neuron* *9*, 1099-1115.

Westenbroek, R. E., Sakurai, T., Elliott, E. M., Hell, J. W., Starr, T. V., Snutch, T. P., and Catterall, W. A. (1995). Immunochemical identification and subcellular distribution of the alpha 1A subunits of brain calcium channels. *J Neurosci* *15*, 6403-6418.

Wettschureck, N., and Offermanns, S. (2005). Mammalian G proteins and their cell type specific functions. *Physiol Rev* *85*, 1159-1204.

Wheeler, D. B., Randall, A., and Tsien, R. W. (1994). Roles of N-type and Q-type Ca²⁺ channels in supporting hippocampal synaptic transmission. *Science* *264*, 107-111.

Wu, L. G., and Saggau, P. (1997). Presynaptic inhibition of elicited neurotransmitter release. *Trends Neurosci* *20*, 204-212.

Yasuda, T., Chen, L., Barr, W., McRory, J. E., Lewis, R. J., Adams, D. J., and Zamponi, G. W. (2004). Auxiliary subunit regulation of high-voltage activated calcium channels expressed in mammalian cells. *Eur J Neurosci* *20*, 1-13.

Zamponi, G. W. (2005). *Voltage-Gated Calcium Channels* (New York, U.S.A., Kluwer Academic/Plenum Publishers).

Zamponi, G. W., Bourinet, E., Nelson, D., Nargeot, J., and Snutch, T. P. (1997). Crosstalk between G proteins and protein kinase C mediated by the calcium channel alpha1 subunit. *Nature* 385, 442-446.

Zamponi, G. W., and Snutch, T. P. (1998). Modulation of voltage-dependent calcium channels by G proteins. *Curr Opin Neurobiol* 8, 351-356.

Zhang, J. F., Ellinor, P. T., Aldrich, R. W., and Tsien, R. W. (1996). Multiple structural elements in voltage-dependent Ca²⁺ channels support their inhibition by G proteins. *Neuron* 17, 991-1003.

Zhou, J. Y., Siderovski, D. P., and Miller, R. J. (2000). Selective regulation of N-type Ca channels by different combinations of G-protein beta/gamma subunits and RGS proteins. *J Neurosci* 20, 7143-7148.

Ziv, N. E., and Garner, C. C. (2004). Cellular and molecular mechanisms of presynaptic assembly. *Nat Rev Neurosci* 5, 385-399.